



## RESEARCH ARTICLE

## A REVIEW ON ELECTROCHEMICAL SUPERCAPACITORS OF COMPOSITE-METAL-OXIDE NANOSTRUCTURES

R.C. Ambare<sup>1</sup>, Rajaram S. Mane<sup>2</sup> B. J. Lokhande<sup>1</sup>.

1. School of Physical Sciences, Solapur University, Solapur 413 255 (M.S.) India

2. Center for Nanomaterials &amp; Energy Devices, School of Physical Sciences, Swami Ramanand Teerth Marathwada University, Nanded, 431 606, India.

**Manuscript Info****Manuscript History:**

Received: 14 January 2016  
 Final Accepted: 26 February 2016  
 Published Online: March 2016

**Key words:**

Composites; Chemical synthesis,  
 Electrochemical properties,  
 Impedance analysis.

**\*Corresponding Author**

R.C. Ambare.

**Abstract**

In near future, use of electrochemical supercapacitors plays important role in energy and power storage applications which are broadly classified into two types; a) electrochemical-double layer capacitors, and b) redox capacitors. Favorable electrode materials used in electrochemical supercapacitors include transition metal oxides, conducting polymers, carbons and their composites etc. Now-a-days the aqueous and non-aqueous chemically grown metal oxide thin film electrodes including ruthenium oxide, iridium oxide, manganese oxide, cobalt oxide, nickel oxide, tin oxide, iron oxide, perovskites, ferrites etc., have been envisaged for electrochemical supercapacitor application. This review presents a brief literature survey regarding electrode materials employed, so far, in electrochemical supercapacitors. Efforts have also been taken to highlight their configurations and charge transport/ collection kinetics.

Copy Right, IJAR, 2016. All rights reserved.

**Introduction:-****Metal oxide-based electrodes:-**

Electrochemical supercapacitors (ESs) exhibit high power density than battery [1]. They are classified into two types; a) electric double-layer supercapacitor (EDLSc) in which charge separation takes place at the surface of electrode and electrolyte interface i.e. non-Faradaic type, e.g. carbon, and b) pseudocapacitors in which charge separation takes place at the surface of electrode i.e., Faradaic reaction. e. g. transition metal oxides.

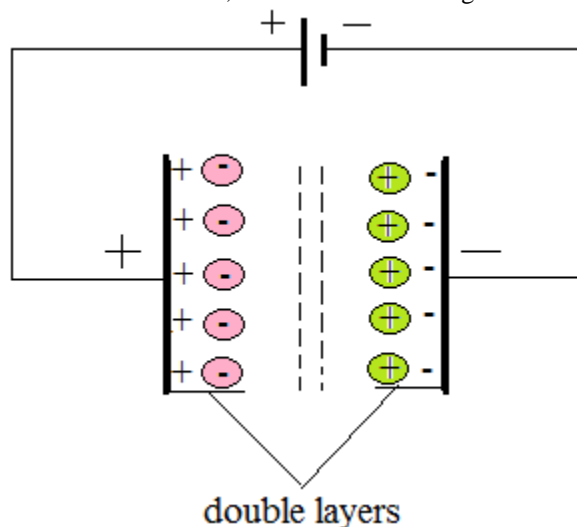


Fig. 1a). Principles of a single-cell double-layer capacitor at the electrode/electrolyte interface.

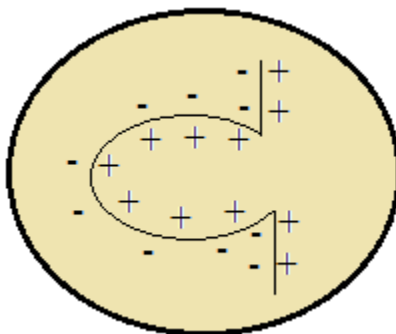


Fig. 1 b) ionic intercalation.

Supercapacitors store excess energy (per unit mass or volume) than a conventional capacitor. The mechanism of energy storage is inherently rapid because it simply involves movement of ions to-and-fro from the electrode surfaces with a very high degree of reversibility in repetitive charge/discharge cycling and demonstrated cycle-life in excess of 500,000. High cycle-life and good chemical or environmental stability make supercapacitors useful in applications such as lightweight electronic fuses, backup power sources for calculators and digital calipers, surge-power delivery devices for electric vehicles etc. Maintenance-free operation of ESs is advantageous over batteries [1, 2].

The capacitance of a device is largely dependent on the characteristics of the electrode material; particularly the surface area and the pore-size distribution, etc [3]. The operating voltage of ESs depends on electrolyte stability. Aqueous electrolytes, such as acids (e.g.,  $\text{H}_2\text{SO}_4$ ) and alkalis (e.g.,  $\text{NaOH}$ ,  $\text{KCl}$ ,  $\text{Na}_2\text{SO}_3$ ,  $\text{Na}_2\text{SO}_4$  and  $\text{KOH}$ , etc.) have the benefit of high ionic conductivity (up to 1 S/cm), low-cost and wide acceptance however; they have the inherent disadvantage of a relatively low decomposition voltage of 1.23 V [4]. Non-aqueous electrolytes allow the use of cell operating voltages above 2.5 V. Non-aqueous electrolyte mixtures such as propylene carbonate or acetonitrile containing dissolved quaternary alkyl ammonium salts can be efficiently applied in many commercial supercapacitors [4]. The electrical resistivity of non-aqueous electrolytes is however at least an order of magnitude higher than that of aqueous electrolyte and therefore, the resulting capacitors generally have a high internal resistance [3]. In ESs, a number of sources contribute to the internal resistance and are collectively measured and referred to as the equivalent series resistance (ESR). Contributors to the ESR of supercapacitors include; (a) overall electronic resistance of the electrode material, (b) the interfacial resistance between the electrode and the current collector, (c) the ionic (diffusion) resistance of ions moving in small pores, (d) the ionic resistance of ions moving through the separator, and (e) the electrolyte resistance [5], etc. The essential ESs electrode need to satisfy desired chemical and physical properties including high conductivity, high surface area, amorphous, nanocrystalline, range (1 to > 2000  $\text{m}^2/\text{g}$ ), good corrosion resistance, high temperature stability, controlled pore structure, processability and compatibility and relatively low-cost, etc [5]. It is possible to fabricate high surface area ESs electrodes that exhibit *Faradaic* electrochemical as well as electrical-double layer type responses. Among the several transition metal oxides and carbon xerogels studied for ESs, the only oxide that has been widely pointed out and known for high superior electrochemical capacitor response to date is the various crystallographic and morphological forms and phases of ruthenium oxide [6]. Unfortunately, the expensive nature of ruthenium is a serious issue before its use in scalability. Alternatively, cost-effective, abundant, chemically non-hazardous and eco-friendly forms and phases of iridium oxide, manganese oxide, cobalt oxide, nickel oxide, tin oxide, iron oxide, perovskites, ferrites, and nanocomposites etc., have been applied in ESs. Generally, two or three electrode system is preferred for ESs where working electrode of polymer, carbon, oxides etc., in thin film form is preferred which can be grown either physically or chemically. The thin film deposition methods involve the growth of these electrodes from the aqueous or non-aqueous solutions are called as chemical or solution methods. Here, a fluid surface precursor undergoes a chemical change at a solid surface, leaving a solid layer. In chemical deposition the solutions contain precursor molecules for a variety of elements in the thin film of interest. These methods are inexpensive and enable to synthesis films of different metal oxides, polymers and organic-inorganic hybrid structures [7]. Depending on applications, one would prefer thin films which have a special texture, low grain boundary density, or smooth surfaces. The methods usually need to have a relatively low operating temperature. Apart from the obvious advantages in terms of energy saving, the use of low deposition temperature that avoids high temperature effects

such as inter diffusion, contamination and dopant redistribution. They offer mysterious morphologies of the thin films which can be easily controlled by preparative parameters. Unlike physical deposition methods, these methods are free from the high quality target and/or substrates. *In justa-pose* they do not in need of any sort of vacuum level, which is one of the great advantages from the point of industrial perspective. Chemical methods include electrodeposition, chemical bath deposition, successive ionic layer adsorption and reaction, electrodeposition, anodization, spray pyrolysis, liquid phase epitaxy, spin coating, dip drying, polymerization, reflex, anodization, etc. This review presents the survey of electrochemical supercapacitive performances carried out based on chemically deposited metal oxide composite material electrodes. It is recorded that these ESs revealed the specific capacitance (SC) values 50 - 1100 F/g, quite comparable with bulk electrode values. Therefore, it is likely that these metal oxide thin films will continue to play a major role in supercapacitor technology.

### Composite electrodes:-

Several efforts have been made on developing ES electrode materials with high capacitances since materials can store more charge, leading to high energy density. These materials store energy through electric double-layer capacitances, faradaic capacitance mechanisms or both. Unfortunately, each one of these materials faces few challenges for example; a) carbon materials may only physically store limited charges, causing low SC, b) conducting polymers may swell and shrink during the intercalating/deintercalating processes leading to low cycling stability, and c) metal oxides may show low specific surface area, poor electronic and ion conductivity limiting the ES power density etc. To address these challenges, composite materials electrodes are introduced as ESs electrode materials. The capacitance of a device is largely dependent on the characteristics of the electrode material particularly, the surface area and the pore-size distribution [8, 9]. In composite electrodes, adding carbon like MWCNT (multiwalled carbon nano tubes), SWCNT and AC (single walled carbon nano tubes), especially carbon nanotubes, into CPs (conducting polymers) is also believed to be an effective solution for improving the mechanical and electrochemical properties of electrodes. It is believed that the composite electrodes help to enhance the cycling stability by improving their chain structure, conductivity, mechanical stability and processability, as well as mitigating mechanical stress.

### Supercapacitive parameters:-

a) Basically, capacitance (C) of material is expressed as  $C = \frac{dQ}{dV}$  (1)

where,  $\frac{dQ}{dV}$  is the rate of charge of surface charge density of the double- layer with electrode potential.

b) Voltage scan rate  $S = \frac{dv}{dt}$  (2)

Therefore,  $C = \frac{dQ}{Sdt}$  (3)

$\frac{dQ}{dt}$  is equal to current I.

where,  $I_1$  and  $I_2$  are the anodic and cathodic current densities ( $I_1$  and  $I_2$  are not in equation).

These CV curves are used to calculate the specific capacitance using the following equations

$$\text{Capacitance } C = \phi_D \frac{I(U) \times d_u}{(2 \times \Delta u \times s \times m)} \quad (4)$$

where, I-V curve is the integral area,  $\Delta u$  is the voltage difference and s, m are the sweep rate and electrode mass.

c) Interfacial capacitance  $C_i = \frac{C}{A}$  (5)

A = is the area of electrode dipped in the electrolyte

d) Specific capacitance  $SC = \frac{C}{W}$  (6)

C= capacitance, W= mass of electrode dipped in the electrode

e) Specific capacitance (SC)

$$C_{sc} = \frac{2 \times I_d \times t_d}{\Delta V \times m}$$
 (7)

$I_d$  and  $t_d$  are discharge current and time (excluding the portion of the sudden potential drop), V = Potential difference (V), m = mass of electrode dipped in the electrolyte (mg).

f) Energy density

It can be calculated by using following relation

$$SE = \frac{CV^2}{2}$$
 (8)

C, V is the specific gravimetric cell voltage and t is the discharge time

g) Specific density

It can be calculated by using following relation

$$SP = \frac{V \times Id}{m}$$
 (9)

h) Efficiency

It is one of the important parameters. Efficiency of the deposited materials depends on charging ( $t_c$ ) and discharging ( $t_d$ ) times which is calculated by using the equation.

$$\eta = \frac{t_d}{t_c} \times 100$$
 (10)

### Electrochemical impedance spectroscopy:-

#### Plot nature:-

EIS is a technique use to measure ESR of a supercapacitor electrode. At lower frequency region ( $Z''$ ) imaginary component use to calculate the capacitance. The EIS “small signal” capacitance is calculated from the imaginary component of the impedance by using the equation [10].

$$C = \frac{1}{-2\pi f Z'' m}$$

(11)

where, C is the EIS signal capacitance, f is lower the frequency (Hz), m is the mass of electroactive material in gm and  $Z''$  the imaginary components in  $\Omega$ . The impedance format emphasizes the values at low frequency, which typically has major interest in electrochemical systems that are influenced by mass transfer and reaction kinetics represents. The impedance of storage devices usually depends on temperature and state of charge. Therefore, sets of impedance spectra have to be analyzed systematically [11–12]. Due to mass transport phenomena, dynamic battery performance during continuous discharging or charging of batteries differs significantly from that during dynamic

microcycling with frequent changes between charging and discharging. As the latter is typical for many practical battery applications (e.g., hybrid-electric vehicles or stop/start vehicles), EIS on Li-ion batteries has been performed using a specific microcycle technique [12]. In the high-frequency range, the SCs show inductive behavior. For intermediate frequencies, the complex-plane plots form an angle of approximately  $-45^\circ$  or  $-90^\circ$  with the real axis. This angle is explained by the limited current penetration into the porous structure of the electrodes (which has been discussed in [13]). For lower frequencies, the spectra approach a nearly vertical line in the complex plane, which is typical of ideal capacitors. Fig.2 shows EIS plot with interpretation.

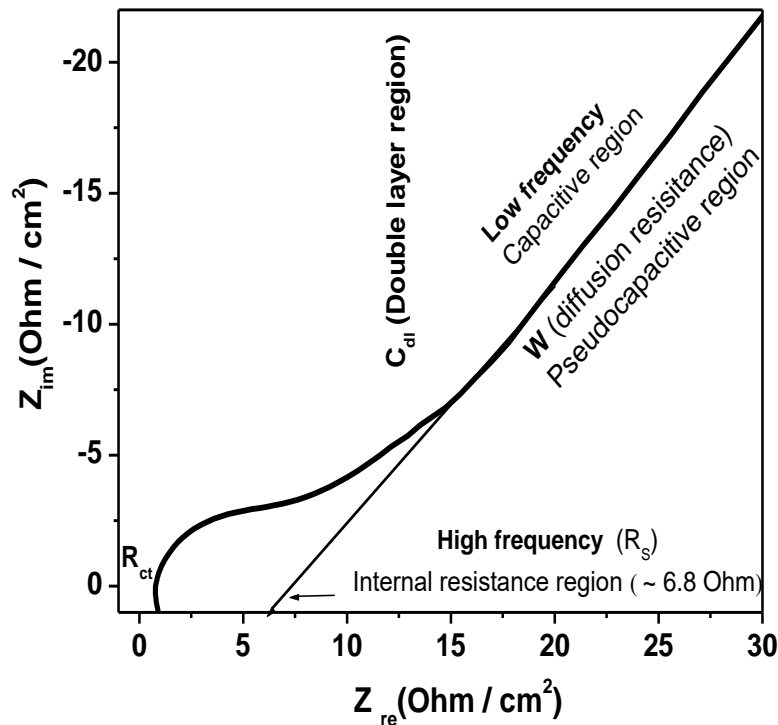


Fig.2 General Nyquist plot.

The study is also associated with bode plot of  $\text{mod } Z$  vs. frequency and  $-\text{phase}$  vs. frequency. In the bode plot magnitude moves towards to impedance as frequency tends toward infinity and toward infinity as  $1/\omega$  as frequency tends towards to zero and phase angle tends towards zero at low frequencies, indicating that the current and potential are in phase [14].

#### Equivalent circuit:-

Simulation-based development methods are increasingly employed to manage with the complexity of modern power electronic systems. For these methods, suitable sub-models of all system components are mandatory. However, compared to the sub-models of most electric and electronic components, accurate dynamic models of electrochemical energy storage devices are rare. Based on the underlying physical processes, the equivalent circuits should allow an optimum representation of the measured spectra with a minimum set of model parameters. In a second step, the model parameters have to be calculated. This circuit consists of an inductance (L), solution resistance ( $R_s$ ), a so-called element representing a depressed semicircle in the complex-plane, charge transfer resistance ( $R_{ct}$ ) [15], a nonlinear RC circuit as well as of (W) Warburg impedance. All relevant processes including porosity, charge transfer and diffusion are modeled with sufficient precision.

### Composite thin film-based ESs:-

The present literature shows the transition metal oxide electrode-based composites for ESs applications are transition metal oxides, polymer and carbon for different composite electrodes etc.

### Transition metal oxide-based composite ESs:-

#### ❖ Cobalt oxide-based composites:-

Cobalt is a low-cost transition metal oxide, deposited in hydroxide/oxide porous forms and envisaged in energy storage application. It is amorphous and *p*-type semiconductor. Various forms of cobalt hydroxide/oxide including nanoflakes, nanorods, nanowires, and spheres with good SC, high redox activity, low stability, high ESR values are documented in literature. The theoretical SC value of cobalt oxide electrode is ~ 3560 F/g [16]. The deposited cobalt oxide required aqueous suitable electrolytes; these electrolytes are less solution resistance, like KOH, KCl, NaOH, Na<sub>2</sub>SO<sub>4</sub>, Na<sub>2</sub>SO<sub>3</sub> etc. Therefore, this aiming is concern to enhance the ESs performance of cobalt oxide electrode by forming the composites with organic, non-metal, inorganic oxide due to their intercalative large potential window, good reversibility, EDLSc and pseudocapacitance properties etc. Lin *et al.* [17] obtained a maximum SC of 291 F/g using CoO<sub>x</sub> xerogel calcinated at 423 K and Srinivasan and Weidner [18] reported the use of Co<sub>3</sub>O<sub>4</sub> film as a positive electrode that exhibited capacitor-like behavior. Wang *et al.* [19] reported Co(OH)<sub>2</sub> electrode with 280 F/g as a single electrode capacitance. The cobalt oxide electrode has been found to have well-efficiency and long-term performance and the good corrosion stability [20, 21]. The Co<sub>3</sub>O<sub>4</sub> thin film prepared by wet chemical method onto conducting and transparent indium-tin-oxide substrate and annealed at 200 °C showed polycrystalline nature and spherical architecture. Electrochemical characterization of prepared anode shows pseudocapacitive behaviour.

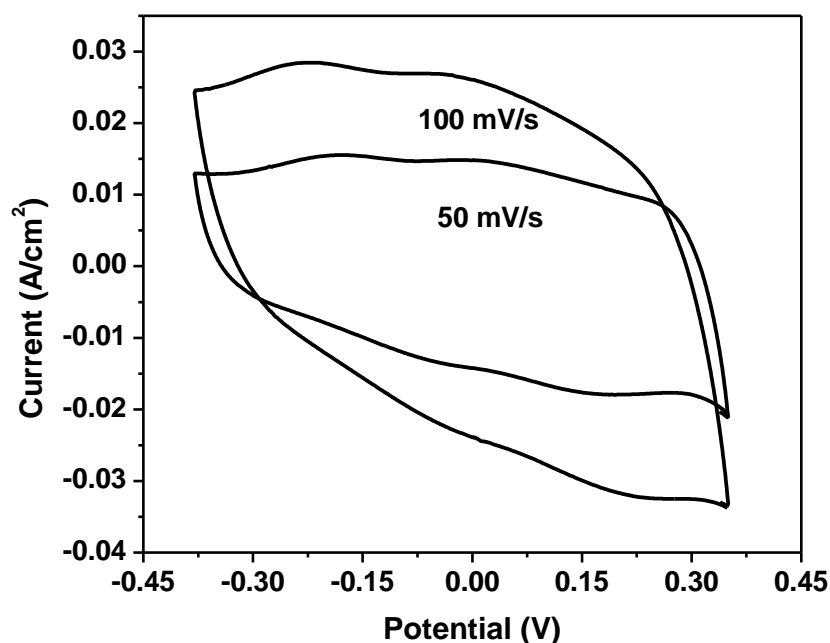


Fig.2 General CVs of Co<sub>3</sub>O<sub>4</sub>.

The SC was calculated using charge discharge test shows 227 F/g at specific current densities 0.2 A/g. The EIS showed internal resistance around 5.5 Ω/cm<sup>2</sup> with slope of ~ 45° [22]. A room temperature, simple and low-cost successive layer adsorption and reaction method for the cobalt oxide film onto copper substrate was developed [23]. Cobalt oxide films were deposited from the cationic precursor CoCl<sub>2</sub> complexed with liquor ammonia solution and the H<sub>2</sub>O<sub>2</sub> as anionic precursor showed SC of 165 F/g in 1.0 M KOH. The composite material was used to decrease the internal resistance and to increase the charge transfer resistance. Cobalt composite electrodes like MWNTs/Co<sub>3</sub>O<sub>4</sub> composites showed a high capacitor property, and the best SC value of 200.98 F/g was obtained which was significantly greater than that of pure MWNTs (90.1 F/g) [24]. Fig.2 shows CVs of ideal rectangular behavior of cobalt oxide.

#### ❖ Ruthenium oxide-based composites:-

Ruthenium oxide is a promising electrode material that exhibits large electrochemical capacitances essential to supercapacitor applications [25–36]. Due to cost of ruthenium, several studies were carried out where it was combined with other materials to form composite electrodes. This was done with the intention to increase the dispersion of ruthenium oxide in other oxide matrix and/or surface [37, 38]. There are lot of RuO<sub>2</sub> composites for example, combination of RuO<sub>2</sub> with other oxides, including VO<sub>x</sub>, TiO<sub>2</sub>, MoO<sub>3</sub>, NiO/RuO<sub>2</sub>, SnO<sub>2</sub> and CaO, RuO<sub>2</sub>/PANi, PPy, carbon/hydrous RuO<sub>2</sub> etc., has resulted in a maximum capacitance of 290 F/g observed for a Ru–V–O composite [39]. Cathodic galvanostatic deposition of RuO<sub>2</sub> on Ni, Ti, Pt and Si foils is accomplished *via* hydrolysis of RuCl<sub>3</sub> by electrochemically generated base [40]. Literature reports that CVs of RuO<sub>2</sub>/TiO<sub>2</sub> electrodes are pseudocapacitive in behaviour. The RuO<sub>2</sub> based composite electrodes shows mixed capacitive behaviour having large potential window 0 to 1.4 V and good value of SC 120 F/g in 1 M KOH. The prepared RuO<sub>2</sub>/TiO<sub>2</sub> composite electrodes shows low internal resistance is 1.5 Ω [41].

#### ❖ Manganese oxide-based composites:-

Manganese oxide including several oxidation states Mn(0), Mn(II), Mn(III), Mn(IV), Mn(V), Mn(VI), and Mn(VII) are used in for manganese oxide-based supercapacitors [42]. The reversibility of these redox transitions is usually too low to be applicable for the supercapacitors although MnO<sub>2</sub>-based electrodes have been employed as the electroactive materials for batteries [43]. Manganese oxide (MnO<sub>2</sub>) provides a relatively lower cost and lower toxicity to that of ruthenium oxide-based supercapacitors. Composite electrodes based of MnO<sub>2</sub> are belonging to carbon nanotubes, carbon blacks, polyaniline and non-metal, inorganic etc. Recently manganese oxides are being considered as potential candidates for electrode material of ESs application [44-51]. The as-prepared MnO<sub>2</sub>-based composite electrode shows symmetric charge discharge curve for numbers of cycle MnO<sub>2</sub>/CNT was also prepared using an inactivated CNT and characterized in an aqueous solution of 1.0M Na<sub>2</sub>SO<sub>4</sub>. The specific capacitances of the MnO<sub>2</sub>/A-CNT composite electrode, measured using cyclic voltammetry at scan rates of 10 and 100mV/s, were found to be 250 and 184 F/g, respectively, compared to 215 and 138 F/g [52].

#### ❖ Nickel oxide-based composites:-

Among transition metal oxides, Ni(OH)<sub>2</sub>, NiO has been widely studied due to its high surface area, high specific pseudocapacitance, and low cost. Furthermore, the theoretical SC value of NiO is 2584 F/g within potential window 0.5 V [53]. Nickel hydroxide and nickel oxide are commonly employed in rechargeable batteries and supercapacitors, owing to their low cost, low toxicity, easy availability, and comparable electrochemical behavior [54]. Due to flowers-type of morphology with high accessible surface area the highest value of SC 703 F/g at potential window 0 to 0.5 V at 2 mV/s scan rate in 6 M KOH electrolyte was reported [55]. In general, a porous structure with a large surface area significantly improves the charge transfer and capacitance of an electrode [56]. NiO shows superior electrochemical behavior when serving as catalyst, electrochromic or battery materials, etc. [57–59]. Two-dimensional (2D), 3D nano-arrays representing an optimized architecture with advantages of high surface to volume ratio, substantial framework structure and open-up geometry exhibited remarkable electrochemical performances [60]. NiO with various morphologies such as nanoparticles [61], nanorods/nanowires/nanofibers [62–65], nanosheets [66], nanotubes [67], flower-like structures [68], hollow spheres [ref] and nanosheet-based NiO microspheres have been synthesized. However, there were few reports about NiO microspheres with different building blocks used in electrochemical capacitors. Nickel oxide electrode for ESs applications shows pseudocapacitive behaviour. The shape of CV curves shows redox peaks with maximum value of SC and small potential window. The prepared electrode itself shows low electrochemical series resistance. The Co(OH)<sub>2</sub>/Ni based composite electrode shows remarkable performance with large potential window – 0.1 V to 0.6 V and high SC 1017 F/g in 2 M KOH. The observed internal resistance from nyquist plot is very low [69].

#### ❖ Iron oxide-based composites:-

Iron oxide, environmentally friendly, is a low-cost, low-ESR, amorphous, nanocrystalline material with pseudocapacitive behavior [70, 71]. Porous Fe<sub>2</sub>O<sub>3</sub> is one of the potential anode materials [72]. Structural, optical electrical and physical properties of Fe<sub>2</sub>O<sub>3</sub> are solution concentration dependent [73, 74]. The iron oxide represents semiconducting behavior [75]. The complete model proposed for the Fe passive film structure in most of the experimental conditions consists on a structure that resembles a spinel Fe<sub>3</sub>O<sub>4</sub> or a defective α-Fe<sub>2</sub>O<sub>3</sub> of closest measured stoichiometry (mostly Fe (III)). Fe (III) displays an *n*-type behaviour, Fe (II) is a highly doped, narrow band gap, *p*-type semiconductor, etc. The main Fe redox transitions on the iron electrode surface result from the availability of free charge carriers at every electrochemical potential [75]. Iron oxide is good oxidizing agent of polymer composites, inorganic, non-metal composites for promising candidates to improve the SC and conductivity

and to decrease the ESR for supercapacitor electrode. Iron oxide-based electrode shows good values of SC with moderate potential window. The prepared electrode itself shows low electrochemical series resistance. The iron oxide based composite electrode shows excellent electrochemical performance with mixed capacitive behaviour, large potential window and excellent SC. The hybrid supercapacitor based on  $\text{MnO}_2$  positive electrode and  $\text{FeOOH}$  negative electrode scanned in  $\text{Li}_2\text{SO}_4$  electrolyte solution was designed. The electrochemical tests demonstrated that the hybrid supercapacitor has a energy density of 12 Whk/g and a power density of 3700 W/kg based on the total weight of the electrode active materials with a voltage range 0 –1.85V. This hybrid supercapacitor also exhibits a good cycling performance and keeps 85% of initial capacity over 2000 cycles [76].

#### ❖ **Copper oxide-based composites:-**

Copper oxide ( $\text{CuO}$ ) is promising pseudocapacitor electrode gives redox process associated with reduction of  $\text{CuO}$  to  $\text{Cu}_2\text{O}$  and *vice-versa*. Maximum SC value of 32 F/g was assigned to  $\text{CuO}$  [77]. It has *p*-type conductivity with narrow band gap 1.2 eV. It possesses low ESR [78] and various forms including like, nanotubes [79], nanostructures [80], nanowires and rods, [81], porous hydrophilic with amorphous [82] with 3D architectures [83] are envisaged in ESs application. Being low-cost material, environmentally friendly, abundant resources, no toxicity and easy preparation [84], it has been enormously used as base material for doping which eventually increases the electrical conductivity of host electrode.  $\text{CuO}$  electrodes are used in rechargeable Li-ion batteries and in heterogeneous catalysts. It has high energy and power density, long cycle life (~ 2000) [84]. Copper oxide-based ( $\text{CuO}/\text{ACNTs}$ ) composite electrodes show improved electrochemical performance with mixed capacitive behaviour and maximum value of SC is 60 F/g in 6 M KOH, good potential window – 1.0 to 0.0 V. The prepared electrodes show nanorods, nanowires type surface morphology which is necessary for supercapacitor [85].

#### ❖ **Vanadium oxide-based composites:-**

Vanadium oxide is another transition metal oxide which has various forms e.g.  $\text{H}_2\text{V}_3\text{O}_8$ ,  $\text{V}_2\text{O}_5$ , and  $\text{V}_6\text{O}_{13}$ . Vanadium oxide shows amorphous, porous, more oxidation state, 3-D network architecture exhibiting very high intercalation reversibility [86]. The  $\text{V}_6\text{O}_{13}$ , has been widely used as cathode material for lithium-ion battery because of their high specific capacitance. It exhibits excellent pseudocapacitance property in organic and aqueous electrolytes [87]. The  $\text{V}_6\text{O}_{13}$  has a blended valence of V (IV) and V (V) which is favorable for increasing the electronic conductivity and these are promising material in supercapacitor electrode [88]. Nanostructured vanadium nitride showed CS value as high as 1340 F/g in 2 mV/s and 554 F/g in 100 mV/s [89, 90]. The multi-oxidation state vanadium oxide prepared composite electrodes itself shows excellent electrochemical performance SC is 180 F/g in 3 M KCl, mixed capacitive behaviour and large potential window (1 V)[91].

#### ❖ **Tin oxide-based composites:-**

A SC of 285 F/g was obtained at a scan rate of 10 mV/ s in 0.1 M  $\text{Na}_2\text{SO}_4$  for nanostructured tin oxide ( $\text{SnO}_2$ ) consisting of many small nanowires, nanorods, porous type morphology. For the same electrode, a SC value of 101 F/g was obtained at a high scan rate of 200 mV/s indicating high-power characteristics of the material. The SC value was increased with the increase in specific mass of  $\text{SnO}_2$ . Reasonably high conductivity of  $\text{SnO}_2$  and the formation of nanostructured and microporous material could be attributed to the high supercapacitive value. A decrease of 2.3% of SC value was observed between 200 and 1000 cycles.  $\text{SnO}_2$  with organic, inorganic and non-metal was prepared for increasing SC value and decreasing the ESR value in high charge storage devices [92-93]. Basically, tin oxide prepared composite electrodes show electrochemical dependent excellent morphologies like nanorods, nanowires and flower. The prepared pristine electrode showed less SC and low potential window and different composite based  $\text{SnO}_2$  electrode approved good supercapacitive performance and good SC value [94].

#### ❖ **Titanium oxide-based composites for supercapacitor:-**

The one-dimensional nanostructured titania ( $\text{TiO}_2$ ) such as nanowires, nanofibers, nanorods, nanoribbons, nanoplates and nanotubes, etc., constitutes an attractive architecture that offers a large surface area and a high structural order [95–98]. Titanium oxide nanotube as a well-designed electrode substrate has attracted considerable interest for energy-storage and various applications such as photocatalysis, environmental protection, etc., due to its porous high accessible surface, electrochemical behavior and chemical stability. Its nanotubular structure also provides more available space for electrochemical reaction [99]. Titanium oxide prepared composite electrode shows electrochemical supported morphologies like, nano tubes, wire etc. Basically, pristine  $\text{TiO}_2$  is a high band gap photo-electrochemical material. The average specific capacitance of nanocomposites with total composite mass from 0.4 to 0.9 mg/cm, measured at 25 mV/s, is about  $400 \pm 25$  F/g ( $545 \pm 35$  F/g based on  $\text{RuO}_2 \cdot x\text{H}_2\text{O}$ ) [100].

#### ❖ Chromium, iridium oxide-based composites:-

Chromium oxide, trivalent chromium as aqueous solution of Cr(III) is significantly less dangerous, in terms of human health and environmental impact, as compared to Cr(VI). To overcome the drawbacks regarding reduction of Cr (III) in aqueous solution, co-deposition of chromium along with metal and the use of specific ligand for Cr<sup>+3</sup> ion are preferred which can generate easily reducible complexes at metal – solution interface [101]. However, capacitance values of chromium oxide are greatly enhanced through pseudocapacitance effects by additional *faradaic* reactions, using nanotubes composites with conducting polymers [102], containing polymers [103] and transition metal oxides [104], etc.

Secondly, iridium oxide (IrO<sub>2</sub>) is an anisotropic material, exhibiting *p*-type character along *c*-axis while *n*-type character along (011) plane. IrO<sub>2</sub> is mostly used in anode material and much superior than that of pure platinum for oxygen evolution [97]. IrO<sub>2</sub> is promising material for O<sub>2</sub> evolution [105], storage devices [106], and activated cathode for H<sub>2</sub> evolution [107]. Different oxidation state chromium oxide electrode showed low SC and small potential window. The capacitance values decrease from 70 F/g at low regime to SC 50 F/g at 5 A/g current loads but preserve still 30 F/g at 50 A/g [108].

#### ❖ Cadmium and zinc oxide-based composites:-

Cadmium and zinc oxide-based electrodes are having less cost and ease to prepare chemically. The CdO electrodes composed of nanowires/nanorods, nanoflakes like morphology electrode demonstrated potential SC values (343 mF/g, 1190 mF/g) in 1 M KOH electrolyte [109, 110]. Zinc oxide (ZnO) is morphology dependent materials with amorphous, porous, nanocrystalline in nature are promising alternative for cost effective materials. The ZnCl<sub>2</sub> activation of bagasse is studied using thermogravimetric analysis and the carbon pore structures are characterized using N<sub>2</sub> and CO<sub>2</sub> adsorption. In two-electrode system, sandwich type supercapacitor cells containing 1M H<sub>2</sub>SO<sub>4</sub> the sugarcane bagasse carbons exhibited specific energy up to 10Wh/kg and specific capacitance close to 300 F/g in 1 M H<sub>2</sub>SO<sub>4</sub> [111]. The as-prepared composite electrode low SC in mF with small potential window?. The specific capacitance of ZnO/CA composite in 6M KOH electrolyte was approximately 25 F/g at 10 mV/s for 2:1 composition. AC impedance analysis reveals that ZnO with carbon aerogel powder enhanced the conductivity by reducing the internal resistance [112].

#### Carbon-transition metal oxide-based composites for supercapacitor:-

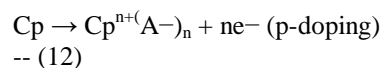
Carbon supercapacitors have been largely investigated because of their low-cost, high cycling-life and high capacitance. Small (few farads) up to large-size (5000 F) devices are commercially available [113]. Highly-porous carbons are used as electrode material due to their high surface area, good electronic conductivity and high electrochemical stability. The most frequently used is activated carbon (1500–2000 m<sup>2</sup>/g). Charge storage is performed through the reversible adsorption of the ions at the active material/ electrolyte interface. No faradic reactions occur during the charge-discharge of the supercapacitor.

Basically, carbon has four crystalline (ordered) allotropes: diamond (sp<sup>3</sup> bonding), graphite (sp<sup>2</sup>), carbyne (sp<sup>1</sup>) and fullerenes ('distorted' sp<sup>2</sup>). While two carbon allotropes are naturally found on earth as minerals, namely, natural graphite and diamond, the other forms of carbon are synthetic. Carbon is considered unusual in the number of its allotropic structures and the diversity of structural forms, as well as in its broad range of physical properties [114]. The attraction of carbon as a supercapacitor electrode material arises from a unique combination of chemical and physical properties, namely; high conductivity, high surface-area range (1 to >2000m<sup>2</sup>/g), good corrosion resistance, high temperature stability, controlled pore structure, processability and compatibility in composite materials, relatively low cost, etc. Pristine carbon prepared electrode shows large potential window with less SC with nearly ideal rectangular behaviour [115].

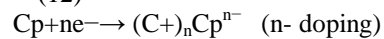
#### Polymer-based composites for supercapacitor:-

Polymers are derived from organic molecules form different monomers like polyaniline, polypyrrole, thiophene/imidazolium, PEDOT etc., [116]. Conducting polymers are generally attractive as they have high charge density and low-cost (compared with the relatively expensive metal oxides). It is possible to develop devices with low ESR, high power, and high energy density. A pseudo-capacitor typically stores a greater amount of capacitance per gram than an EDLC, as the bulk of the material (not just the surface layer) reacts. On the other hand, an EDLC has faster kinetics as only the surface of the carbon is being accessed. An example of a pseudocapacitive material is a conducting polymer (CP) (the conductivity of which was first reported in 1963 by Weiss and co-workers in Australia [117–120].

Conducting polymers can be *p*-doped with (counter) anions when oxidized and *n*-doped with (counter) cations when reduced. The simplified equations for these two charging processes are as follows:



-- (12)



-- (13)

The discharge reactions are, of course, the reverse of the above equations.

Polymers are *p*-type conductivity, excellent morphologies, and pseudocapacitive behaviour with low stability. The composite prepared electrode shows nearly rectangular in nature with improved electrochemical life cycle, high value of SC, low internal resistance. [121].

**Table 1** Transition metal oxide-based composites used for supercapacitors.

Sr. No Ref.	Deposition method and Conditions	Film properties Electrode	Electrolytes	SC (F/g)	SE Wh/kg	SP kW/kg	$\eta$ %	Impedance configurations
[122]	<u>Chemical co-precipitation</u> Substrate: Ni:Co:Mn = 1:1:1 Was dissolve in 100 mL DW, 5 % ammonium hydroxide pH = 9.5 vigorous stirring. Potentiodynamic: -0.1- +0.45 V/s, scanning rate 5; 10; 20 mV/s, annealing	Mn-Ni-Co oxide	6 M KOH	1260	--	--	--	frequency rage $10^5$ to $10^{-2}$ Hz, $R_i = 0.43 \Omega$ .
[123]	<u>Anodization process</u> Substrate: TiO <sub>2</sub> /Ti, HF (3.3) - HNO <sub>3</sub> (5.6), Anode -Ti, Cathode - RuO <sub>2</sub> Galvanostatic ED At current -1.0 mA/cm <sup>2</sup> for 30 min.0.02 M RuCl <sub>3</sub> and 0.005 M (HCl) scanning rate 10 mV/s, annealing at 298 K.	RuO <sub>2</sub> - TiO <sub>2</sub> /Ti nanotubes	1 M H <sub>2</sub> SO <sub>4</sub>	640	128.0	2.4	--	frequency rage 0.01to100 kHz,
[124]	<u>Co-Sputtering method</u> Substrate: Si wafer, Sweep rate 10 and 5 mV/s, PD: 0 to 1V.	SnO <sub>2</sub> - RuO <sub>2</sub>	0.5 M H <sub>2</sub> SO <sub>4</sub>		1.72 $\times 10^{-5}$ Wh/cm <sup>2</sup>	24.6	--	--

[125]	<u>Potentiostatic deposition</u> Substrate: TiO <sub>2</sub> /Ti, HF (3.3)- HNO <sub>3</sub> (5.6), At current -1.0 mA/cm <sup>2</sup> for 30 min. 0.02 M RuCl <sub>3</sub> and 0.005 M (HCl) scanning rate 10 Potentiodynamic: - 0.1 to +0.6 V mV/s, annealing at 298 K.	Co <sub>x</sub> Ni <sub>1-x</sub> LDHs dense microstructure	1 M KOH	2104	--	--		frequency rage 0.01to100kHz, Ri =0.05 Ω for Co Ri =1 Ω for Ni with 45 <sup>0</sup>
[126]	<u>Hydrothermal synthesis</u> Substrate: Nickel foam 5mmol cobalt acetate, 15 mmol hexamethylenetetramine in 50 ml DW, electrodeposition of Ni 2 mA/cm <sup>2</sup> for 240 s, M NiCl <sub>2</sub> , 0.05 M, H <sub>3</sub> BO <sub>3</sub> and 0.2 M Ethylenediamine dihydrochloride scanning rate 10 mV/s PD: - 0.2 to + 0.6 V	Co (OH) <sub>2</sub> / Ni Porous, nanoflake	2 M KOH	1310	--	--	--	frequency rage 0.01Hz to100 kHz,
[127]	<u>Electrochemical deposition</u> Substrate: stainless steel Annealed at 300 <sup>0</sup> C for 3 h, PD: - 0.7- + 0 V Ag/AgCl. scanning rate 100 mV/s	Co – Ni / Co – Ni nanocrystalline Cauliflower	1 M KOH	331	--	--	--	frequency rage Ri = 0.4 Ω
[128]	<u>Chemical precipitation method</u> Substrate: glassy carbon cobalt nitrate + nickel Nitrate (1:1M) dry at 100 <sup>0</sup> C, scanning rate 1; 5; 10; 20; 50 mV/s, PD: 0 – 1.5 V Ag/AgCl.	Ni and Co oxide Thin flake	1 M NaOH 0.5 M Na <sub>2</sub> SO <sub>4</sub>	1840	--	--	---	--

[129]	<u>Cyclic voltammetry method</u> Substrate: titanium, Rh(NO <sub>3</sub> ) <sub>3</sub> and Co(NO <sub>3</sub> ) <sub>2</sub> .xH <sub>2</sub> O 6.0 mol/dm <sup>3</sup> , by addition of NaOH, Sample annealed at 400 <sup>0</sup> C for 1 h, scanning rate 20 mV/s, PD: 0.3 to 1.5 V Ag/AgCl.	Ti/RhO <sub>x</sub> + Co <sub>3</sub> O <sub>4</sub> cracked - mud	0.5 M H <sub>2</sub> SO <sub>4</sub>	800	--	--	---	--
[130]	<u>Chemical reduction method</u> Substrate: Ni foam Co- B alloy (0.3g) in 10 ml of DW Sample annealed at 500 <sup>0</sup> C for 1 h, Scanning rate 0.2 mV/s, PD: - 1.2 -- - 0.4 V Hg/HgO.	Co – B - Carbon nanoflakes	6 M KOH	430 mAh/g 100 cycle	--	--	10 <sup>4</sup> to 10 <sup>-1</sup> Hz V = - 1.0 V, R <sub>ct</sub> = C <sub>1</sub> to C <sub>4</sub> 0.325 Ω , and 0.188 Ω 0.144 Ω , 0.102 Ω	
[131]	<u>Hydrothermal method</u> Substrate: Ni foam 200 mg Co(NO <sub>3</sub> ) in 5ml of DW heated at 180 <sup>0</sup> C for 1.5 h, current densities 0.4 to 3 A/g. GS mode	Co <sub>3</sub> O <sub>4</sub> @graphene nanoflakes	6 M KOH	415 F/g 3 A/g	--	--	--	--
[132]	<u>Chemical precipitation method</u> Substrate: Ni foam NH <sub>4</sub> NO <sub>3</sub> at 35 <sup>0</sup> C for 14 h, Steaming at 650 <sup>0</sup> C for 3h, 30mL NH <sub>3</sub> .H <sub>2</sub> O (5 ml 25-28 wt %) Added dropwise CoCl <sub>2</sub> .6H <sub>2</sub> O (0.0126 M, 24.79 wt.%), pH~8.5. Heated at 100 to 450 <sup>0</sup> C for 3h	Co graphene SEM, TEM.	1 M KOH	958 F/g	--	--	--	--

[133] <u>Chemical vapour deposition</u> Substrate: graphite 2M Ni(NO <sub>3</sub> ) <sub>2</sub> and 1 M Co(NO <sub>3</sub> ) <sub>2</sub> Ni/Co molar ratios was in CNT/graphite Electrode by micro-syringe, heated at 250 <sup>0</sup> C for 2h, current densities 0.4 to 3 A/g. GS mode	Cobalt -Nickel oxides/carbon nanotubes	1 M KOH	569 F/g	--	--	--	--
[134] <u>Electrodeposition</u> Nanocrystalline, nano plates PD= - 0.2 to 0.6 V,	NiCo2O4@NieS	1 M NaOH	926 F/g	--	--	--	--
[135] <u>Co-Precipitation method</u> Substrate: Ti foil Nickel acetate tetra hydrated Cobalt(II) acetate tetra hydrated In glacial acetic acid + activated Carbon powder addition of oxalic acid, In water/iso propanol, centrifuge and dried, 80 <sup>0</sup> C and calcinated at 400 <sup>0</sup> C. PD: - 0.2 to 1.2 V,	Cobalt -Nickel	1 M KCl	59 F/g 4 mV/sec	0.06 Wh/kg	975 W/kg	86.7 %	impedance
[136] <u>Cyclic Voltammetric method</u> Glassy carbon, Ni(SO <sub>4</sub> ). 7 H <sub>2</sub> O, CoSO <sub>4</sub> . 8 H <sub>2</sub> O Boric acid, sodium hydroxide and methanol. PD: 100 and 700V.	Nickel – Cobalt	0.1 M NaOH		--	--	--	Impedance

[137] <u>Chemical Bath Deposition</u> Substrate- ITO, Ni(NO <sub>3</sub> ) <sub>2</sub> . 6 H <sub>2</sub> O, CoCl <sub>2</sub> . 6 H <sub>2</sub> O, KOH, Ammonia, Annealed at 300 <sup>0</sup> C for 1h, PD: 0 to 0.5 V (Ag/AgCl).	Nickel – cobalt	2 M KOH	NR- NF -	490 330 F/g	45 19 Wh/kg, kW/kg	2	--	--
[138] <u>SILAR Method</u> Stainless steel, 0.1 M CoSO <sub>4</sub> and 0.1M NiSO <sub>4</sub> pH~ 12, H <sub>2</sub> O <sub>2</sub> was kept at 343 K PD: 0 to 500V,	Nickel – cobalt	2MKOH		672 F/g	--	--	--	10 <sup>-3</sup> to 10 <sup>3</sup> 0.47 Ω
[139] <u>Chemical co-precipitation</u> MnO electrode, Synthesis of MNCO Stoichiometric amount (1:1:1) Preparation of MNCO electrode 0.2M thiourea + 0.1 M manganese Chloride PD= 0 to 500V.	Mn-Ni-Co oxide	6MKOH 1000 cycles stability		1260 F/g	--	--	--	10 <sup>-2</sup> to 10 <sup>5</sup>
[140] <u>Polymerizable- complex Method</u> Stainless steel, mix of RuCl <sub>3</sub> .n H <sub>2</sub> O, VO(OC <sub>3</sub> H <sub>7</sub> ) <sub>3</sub> Citric acid, CH <sub>3</sub> Scanning range- PD= 0 to 500V.	Ru <sub>1-x</sub> V <sub>x</sub> O <sub>2</sub>	2MKOH		672 F/g	--	--	--	--
[141] <u>DC Sputtering</u> Pt/Ti/Si, 0.5 M H <sub>2</sub> SO <sub>4</sub> RuO <sub>2</sub> -SnO <sub>2</sub> composite	RuO <sub>2</sub> -SnO <sub>2</sub> nanocrystalline amorphous TEM, TED	0.5 M H <sub>2</sub> SO <sub>4</sub>		62.2 F/g	--	--	--	--

Scanning – 10 mV/sec,  
PD-0 to 1000

[142]	<u>Electrodeposition</u> ITO 0.05 M Ti(III) Cl <sub>3</sub> HCl, 1:2, 0.04 M ruthenium Chloride, pH~2 and 5 Deposition was at 313 K, PD- 0 to 1000, anodic potential + 1 V, Scanning – 10 mV/sec. PD- 600-0 (Ag/AgCl)	TiO <sub>2</sub> -RuO <sub>2</sub> TEM, SED pattern thickness 0.0014 to 0.0059 g/cm <sup>2</sup>	0.5 M H <sub>2</sub> SO <sub>4</sub>	788 F/g	--	--	--	--
[143]	<u>Sol – Gel Method</u> PVA- H <sub>3</sub> PO <sub>4</sub> , H <sub>2</sub> O Product was dried At 105 <sup>0</sup> C, Scanning – 5mV/sec. PD – 0.2 to 1V.	RuO <sub>2</sub> -TiO <sub>2</sub> nanotubes	1 M KOH	1263 F/g	--	--	--	10 <sup>5</sup> to 10 <sup>-2</sup> Hz 1.5 – 2 Ω
[144]	<u>Potentiostatic Anodization</u> Ti metal, 0.15M HF, 0.5 M H <sub>3</sub> PO <sub>4</sub> nanotubes, Annealing treatment , 450 <sup>0</sup> C for 2h, 0.1 M sodium dodecyl , benzene Sulfate ethanol, Chloride, pH~2 and 5, Finally heated at 300 <sup>0</sup> C for 2h, Deposition was at 313 K, PD- 0.9 to 0.9, Scanning – 10 mV/sec, PD- 600-0 (Ag/AgCl).	NiO - TiO <sub>2</sub> flower like	1 M NaOH	46 mF/cm <sup>2</sup>	--	--	--	--

**Table 2: Carbon–transition metal oxide-based composites used for supercapacitors.**

Sr. No	Deposition method and	Film properties	Electrolytes	SC (F/g)SE	SP	$\eta$	Impedance		
Ref.	Conditions					Wh/kg	kW/kg	%	configurations
[145]	Thermal decomposition RuO <sub>2</sub> .xH <sub>2</sub> O and sodium Ethoxide were mixed In ethanol and stirred at 70 <sup>0</sup> C for 3 h, scanning rate 10 mV/s PD: 0 - 1 V.	Carbon / hydrous RuO <sub>2</sub> Porous, granular particles	1 M H <sub>2</sub> SO <sub>4</sub>	1017	--	--	--	frequency rage 0.01Hz to100 kHz R <sub>ct</sub> = 0.3- 0.8 $\Omega$ slope 45 <sup>0</sup>	
[146]	Hydrothermal method NH <sub>4</sub> VO <sub>3</sub> (0.8) Calcinated at 500 <sup>0</sup> C 3h SnO <sub>2</sub> - V <sub>2</sub> O <sub>5</sub> NH <sub>4</sub> VO <sub>3</sub> (0.05 M) SnCl <sub>2</sub> .2H <sub>2</sub> O (0.05 M) 250 ml DW, urea: (0.2 M) scanning rate 100 mV/s Potentiodynamic: 0 - 1 V.	V <sub>2</sub> O <sub>5</sub> , V <sub>2</sub> O <sub>5</sub> - CNT, SnO <sub>2</sub> - V <sub>2</sub> O <sub>5</sub> , SnO <sub>2</sub> - V <sub>2</sub> O <sub>5</sub> - CNT, Porous, granular particles	1 M KCl121.4		--	--	--	--	
[147]	Co-Precipitation method MWCNTs	Co <sub>3</sub> O <sub>4</sub> /MWCNT Porous ,	1 M KOH	418	--	--	--	frequency rage R <sub>ct</sub> =	

	Conc. nitric acid at, 140 <sup>0</sup> C, Prepared 20 mg MWCNTs, + 50 ml of CoCl <sub>2</sub> .6 H <sub>2</sub> O, Molar conc. (0.14, 0.082, 0.057 and 0.024), scanning rate, 10, 20, 30, 40, 50 mV/s, PD: - 0.3 – 0.6 V.	granular particles pore size 2 to 10 nm						0.87- 0.71 Ω slope 45 <sup>0</sup>
[148]	Chemical impregnation 1M NH <sub>4</sub> HCO <sub>3</sub> + RuCl <sub>3</sub> / ACB, annealed at 150 <sup>0</sup> C, For 2 h, scanning rate, 2, 5, 10, 25, 50 mV/s, PD: - 0.8 – 0.8 V.	Hydrous RuO <sub>2</sub> /ACB amorphous hydrous FE-SEM, small particles pore size 50 nm	1 M H <sub>2</sub> SO <sub>4</sub>	1255.8 F/g	--	--	--	--
[149]	Co-Precipitation method Nickel (II) acetate tetra hydrate + glacial acetic acid + addition of oxalic acid centrifuge and dried 80 <sup>0</sup> C calcinated at 400 <sup>0</sup> C, scanning rate 4, 20, 50, 100, 200 mV/s. PD: 0 – 1.0 V (Ag/AgCl).	Ni-Co oxide/ AC, TEM, spinal phase crystalline size 25.7 – 8.5 nm	1 M KCl59	0.06 F/g	975	--	frequency rage W/kg	slope 45 <sup>0</sup>

[150]	Microwave assisted 1.28 g of cobalt Nitrate hex hydrated And 1.32 g urea, In 200 mL centrifuge and dried 80 <sup>0</sup> C calcinated at 400 <sup>0</sup> C, of GO suspension (0.5mg /mL), dry at 100 <sup>0</sup> C, calcinated at 320 <sup>0</sup> C for 1h, scanning rate 10, 20, 50, 100 mV/s, PD: 0 – 0.4 V (vs SCE).	GNS/CO <sub>3</sub> O <sub>4</sub> nanoparticle 3 – 5 nm, spinal phase crystalline size	6 M KOH F/g	243.2	--	--	--	frequency rage 100 kHz to 0.1 Hz OCP= 5mV, slope 45 <sup>0</sup> Rct=1.66 to 5.063 Ω
[151]	Cyclic voltammetric NiSO <sub>4</sub> . 7H <sub>2</sub> O, CoSO <sub>4</sub> .8 H <sub>2</sub> O + Boric acid, sodium hydroxide and methanol Glassy carbon disc = Ni/Co ratio= 1:1, 2:1, 3:1, 4:1, Working electrode, pH=2, scanning rate 20 mV/s, Potc: -1050 – 50 mV (vs Ag/AgCl).	Ni-Co S=glassy carbon nanoparticle, 3 – 5 nm crystalline size .	0.1 M NaOH	243.2	--	--	--	frequency rage 100 kHz to 0.1 Hz
[152]	Chemical vapor deposition 2 M Ni(NO <sub>3</sub> ) <sub>2</sub> and 1M Co(NO <sub>3</sub> ) <sub>2</sub> , Carbon	Ni - Co oxide NiO, Co <sub>3</sub> O <sub>4</sub> S=graphite	0.1 M KOH	569	--	--	--	--

	Nanotubes (Ni/Co: different molar ratio) heat at 250 <sup>0</sup> Cfor 2h, 2000 <sup>th</sup> C-D cys. scanning rate 10 mA/cm <sup>2</sup> , Potc.: o – 0.5 V (vs SCE).	SEM: nanotubes						
[153]	Screen Printing 0.3 M zinc acetate 0.3 M tin acetate, Dt : 430 <sup>0</sup> C scanning rate 50 mV/s, Potc.: - 0.6 to 0.6 V (vs SCE).	G – ZnO G – SnO <sub>2</sub> S=graphite, TEM, FESEM: grain spreading in a large - scale.	0.1 M KCl 61.7		--	--	--	0.1 Hz to 100 kHz Rct- G-ZnO / SnO <sub>2</sub> 1.5, 0.6 Ω G= 2.5 Ω ESR : 1.86,2.23, 3.34 Ω
[154]	Hydrothermal reaction 2 M Ni(NO <sub>3</sub> ) <sub>2</sub> and 25 mL of 0.1 mol/L KMnO <sub>4</sub> scanning rate 0.1 A/g.	MnOOH nanowire graphene oxide	1 M Na <sub>2</sub> SO <sub>4</sub> 76		--	--	--	0.01 Hz to 100 kHz 45 <sup>0</sup>
[155]	Chemical Precipitation K <sub>0.14</sub> MnO <sub>2+y</sub> 0-20 wt% MWCNT With total mass of 40 mg/cm <sup>2</sup> Scanning rate 2 mV/sec.	Manganese dioxide MWCNT	0.5 M Na <sub>2</sub> SO <sub>4</sub>	155	--	--	--	100 MHz to 70 kHz 45 <sup>0</sup> ~ 0.5 Ω /cm <sup>2</sup>

[156]	Spray Pyrolysis MWCNT PD - Scanning rate 25 mV/sec.	Carbon nanotubes Manganese oxide	1 M Na <sub>2</sub> SO <sub>4</sub>	228		--	--	--	--
[157]	Hydrothermal Method MWCNT 0.1 M KMnO <sub>4</sub> & 0.1M K <sub>2</sub> SO <sub>4</sub> , Scanning rate 2 mV/sec. PD = 0 to 1V.	Graphene/ MnO <sub>2</sub>	1 M Na <sub>2</sub> SO <sub>4</sub>	211.5		--	--	--	10 <sup>5</sup> to 0.1 Hz OCP=5 mV
[158]	Electrodeposition CNT and Permanganate ions Scanning rate 1 mV/sec, PD -2 to 4.5 V.	LiMnO <sub>4</sub> MnO <sub>2</sub> /CNT	1 M LiClO <sub>4</sub>	MnO <sub>2</sub> /Ac	52	26	2400	--	--
				MnO <sub>2</sub> /MNT			56	Wh/kg	W/kg
							F/g		
[159]	Potentiodynamical Method Pb substrate 0.5 M/L, MnSO <sub>4</sub> , and 0.5 M/L H <sub>2</sub> SO <sub>4</sub> , mixed Scanning rate 10 mV/sec. PD = - 0.8 to 0.8V.	Manganese oxide/ Carbon crystalline, rough, higher surface area	1 M Na <sub>2</sub> SO <sub>4</sub>	410		--	--	--	10mHz to10K Hz OCP=5 mV

[160]	Chemical impregnation 1M ammonium hydrogen Carbon, in to aqueous RuCl <sub>3</sub> /ACB solution Composite were annealed At 150 <sup>0</sup> C for 2h. Scanning rate 2-50 mV/sec. PD -2 to 4.5 V.	RuO <sub>x</sub> /ACB	1 M H <sub>2</sub> SO <sub>4</sub>	1255 533.7	--	--	--	--
[161]	Sol – Gel Method Pb substrate 5 g, RuCl <sub>3</sub> , and 0.27 M/dm <sup>3</sup> HCl, Composite was dried At 110 <sup>0</sup> C for 24 h. Scanning rate 10 mV/sec. PD = - 0.8 to 0.8V.	RuO <sub>2</sub> / Carbon black crystalline, rough, higher surface area	1 M H <sub>2</sub> SO <sub>4</sub>	20	--	--	--	10 mHz to 10K Hz 120 Ω for X <sub>c</sub> 170 Ω for X <sub>c</sub> / 46
[162]	Hydrothermal Method V <sub>2</sub> O <sub>5</sub> by solid state NH <sub>4</sub> VO <sub>3</sub> , alumina Crucible, Sn.Cl <sub>2</sub> .2H <sub>2</sub> O Calcinated at 500 <sup>0</sup> C for 3h. At 110 <sup>0</sup> C for 24 h. SnO <sub>2</sub> -V <sub>2</sub> O <sub>5</sub> by hydrothermal pH~8, Scanning rate 0.1V/sec. anodic,	SnO <sub>2</sub> -V <sub>2</sub> O <sub>5</sub> CNT V <sub>2</sub> O <sub>5</sub> -CNT, SnO <sub>2</sub> -V <sub>2</sub> O <sub>5</sub> -CNT	0.1 M KCl	7.65 2.40 26.28 121.39	--	--	--	--

	PD = 0.0 to 0.8V.									
[163]	Sol – Gel Method	V <sub>2</sub> O <sub>5</sub> /	Carbon	2-3 M LiClO <sub>4</sub>	120	26	80	--	--	--
	Ni foam substrate		SEM- roughly			mA h/g	kW/kg,	h/kg		
	V <sub>2</sub> O <sub>5</sub> by sol		spherical							
	Composite prepared by sol									
	Scanning rate 0.035,									
	0.7 V/min. PD = 1 to 5 V.									
[164]	Chemical Vapor deposition	CMK-3/Carbon	6 M KOH	208	10	--	--		10 kHz to 4 mHz	
	0.3g Fe (NO <sub>3</sub> ) <sub>3</sub> for 80 <sup>0</sup> C	SEM- porous		F/g	kW/kg				10 mV	
	Fe/Si atomic ratio									
	CVD was 850 <sup>0</sup> C for 90 min,									
	50 mL of 20% hydrofluoric acid									
	Dried at 100 <sup>0</sup> C for 24h,									
	Scanning rate 0.035, 0.7 V/min.									
	PD = 1 to 5 V.									
[165]	Chemical Method	GNs/SnO <sub>2</sub> -MWCNT	6 M KOH	224	17.6	31	81		100 kHz to 10MHz	
	Nitric acid (5 N)	SEM- porous		F/g	kW/kg,	Wh/kg,	%		10 mV	
	At 60 <sup>0</sup> C for 4h, in DW,									
	10 mg of MWCNT in 40 ml									
	DW and 1 g of hydrous SnCl <sub>2</sub>									
	Dried in 90 <sup>0</sup> C for 6h and									
	calcinated at 350 <sup>0</sup> C for 2h,									
	Scanning rate 5 – 200 m V/sec,									
	PD = 1 to 5 V.									
	GS = 0 and +1 V.									

[166]	Electro spun Nickel acetate tetra, hydrated ruthenium, porous actetylacetone mixed with 10 % polyacrylonitrile, N, N – dimethyle-formamide, to maintain the wt% of nickel acetate, NiRu-C-NF-O, NiRu-C-NF-1, NiRu-C-NF-2, Scanning rate 0.058m V/s, PD = 0.0 to 3 V.	NiO/ RuO <sub>2</sub> SEM- nanowire	6 M KOH F/g	~ 60	--	--	--	0.18MHz to 36 mHz internal resistance
[167]	Co- Precipitation MWCNT, ferric chloride Ammonium hydroxide Conc. sulfuric acid and nitric acid (1:3 v/v) at 80 <sup>0</sup> C, starring for 6h With reflex, pH neutral Fe <sub>2</sub> O <sub>4</sub> / MWCNT composites Scanning rate 0.035, 0.7 V/ min. PD = - 0.8 to 0.0 V.	Fe <sub>3</sub> O <sub>4</sub> /MWCNT 1 M Na <sub>2</sub> SO <sub>3</sub> SEM-TEM, HRTEM XPS- BE= 711 eV	MWCNT=58 Fe <sub>3</sub> O <sub>4</sub> / MWCNT = 165 F/g in 0.2 A/g 1000 cycles 103 F/g	--	--	--	--	

**Table.3: Polymer-based composites used for supercapacitors.**

[168]	Chemical Method	PSDOT/CNTs	1 M H <sub>2</sub> SO <sub>4</sub>	100 to 330	--	--	--	---	
	0.5 M, pyrrole	nanotubes diameter							
	1.2 g of FeCl <sub>3</sub> , +	10 to 15 nm,		F/g					
	50 ml of 0.1 M/L	SEM: porous							
	PANi/CNTs								
	0.4 g K <sub>2</sub> Cr <sub>2</sub> O <sub>7</sub> in 50 M/L HCl								
	dry at 60 <sup>0</sup>								
	scanning rate 10 mV/s,								
	Potc.: - 0.8 to 0.4 V								
	(vs Hg/Hg <sub>2</sub> SO <sub>4</sub> ).								
[169]	Sol-Gel	PSDOT/CNTs	1 M H <sub>2</sub> SO <sub>4</sub>	305.3	42.4	--	96	0.1 Hz to 10 kHz	
	Inorganic-organic	nanocrystalline		F/g			%	Ri = 0.08 Ω	
	SnO <sub>2</sub> + aniline	20 to 60 nm,						45 <sup>0</sup>	
	2g SnCl <sub>2</sub> . 2 H <sub>2</sub> O	SEM: micro-porous							
	In 100 ml ethanol								
	dry at 120 <sup>0</sup>								
	Calcination : 400 <sup>0</sup> C for 2h								
	PANi- SnO <sub>2</sub> sodium dodecylben								
	Sulfonate 4 g in 1 M HCl (70 ml),								
	SnO <sub>2</sub> (0.5 g), aniline 5 m mol,								
	Stirring: 1 M HCl (30 ml containing APS 5mol)								
	Cooled at 0-5 <sup>0</sup> C stirring at 6 h,								
	Filter add 1M HCl , ethanol dry 50 <sup>0</sup> C.								
	scanning rate 5 to 50 mV/s,								

	PD.: - 0.2 to 0.8 V (vs SCE).							
[170]	Chemical Oxidation Polymerization	PANi/neutral red 1 M H <sub>2</sub> SO <sub>4</sub>	335	--	--	--	Frequency range	
	Aniline, NR,(NH <sub>4</sub> ) <sub>2</sub> S <sub>2</sub> O <sub>8</sub> ,	TiO <sub>2</sub>	5 mA (G)				0.01 to 10 <sup>5</sup>	
	Titanium nano powder	PANi/PNR/TiO <sub>2</sub>					5 mV, 45 <sup>0</sup>	(~ 25
	nm) and H <sub>2</sub> SO <sub>4</sub>	XRD: amorphous for PANi					R <sub>ct</sub> : PANi/PNR and	
	PANi/PNR/TiO <sub>2</sub>	polycrystalline for PANi/PNR/TiO <sub>2</sub>					PANi/PNR/TiO <sub>2</sub>	
	0.2 g TiO <sub>2</sub> + aniline						0.6 and 0.3 Ω	
	In 200 ml 1M HCl mixture is in							
	Ice water bath (0 - 5 <sup>0</sup> C), vacuum at 60 <sup>0</sup> C.							
	scanning rate 1, 2, 5, 10, 50 in mV/s,							
	Potc.: - 0.2 to 0.8 V,							
	(vs SCE).							
[171]	Rapid mixed reaction	PANi/CNTs	30 wt% KOH	163	--	--	--	---
	3. g ammonium per sulfate	nanocrystalline	0.1 A/g					
	1.09 aniline monomer	10 to 15 nm,						
	In 60 ml DW	SEM: porous						
	Starring at r t., f or 24 h							
	dry at 120 <sup>0</sup>							
	Calcination: 400 <sup>0</sup> C for 2h							
	Centrifuge, Sample annealed at different							
	Temperature, scanning rate 5, 10, 20, 50, 100 in mV/s,							
	Potc.: - 0.85 to 0.01 V, (vsHg/HgO).							

[172]	Chemical Polymerization method CMK-3 1 g in 20% ethanol Solution containing 2.8 g Aniline, 20 g H <sub>2</sub> SO <sub>4</sub> Starred under vacuum for 1 h, Aniline/APS ratio 1:2.3 was added, At 0 <sup>o</sup> C for 5 h, Electrode: 8 mg em + 0.75 mg, Acetylene black and 0.75 mg graphite, 0.05 mg poly(tetrafluoroethylene) + ethanol, dry at 353 K for 16 h in air, scanning rate 5, 10, 20 in mV/s, PD.: 0 to 1.4 V.	PANi/CMK-3 SEM: porous irregular big particle	1M H <sub>2</sub> SO <sub>4</sub>	87.4 1000	23.8 5 mA/cm <sup>2</sup> 1000 cycle	206 kW/kg	90 W/kg	---	
[173]	Synthetic method GO and PANI, AC prepared Electrode Carbon black + poly (tetrafluoroethylene) Mass ratio (85: 10: 5), Nickel foam, Dry 100 <sup>o</sup> C for 12 h, Scanning rate 1 to 200 in mV/s, PD.: - 1 to 0.0 V (Hg/HgO SCE).	PANi/CMK-3 SEM: mesopore, surface area: 1976 m <sup>2</sup> /g.	6M KOH	455	1 mV/s	--	--	--	---

[174]	CVD CNTs and PPy 0.1 M PBS with a pH scanning rate 25, 50 and 100 in mV/s, PD.: - 0.5 to 0.5 V (Ag/AgCl).	PPy/CNTs SEM: nanowire, XPS and TEM	3 M KCl 0.1 M pyrrole + 0.1 M NaClO <sub>4</sub>	1587 F/g	--	--	--	0.01 to 10 <sup>5</sup> Hz 45 <sup>0</sup>
[175]	Electro polymerization CNTs and PPy tantalum electrodes. EDOT (Baytron, 99%) and Py scanning rate 2 to 200 mV/s, PD.: - 0.6 to 0.8 V (SCE).	PEDOT/PPy (5:1) FE SEM: highly, Porous horn-like structure	1 M KCl 1M LiClO <sub>4</sub>	230 290 100 mv/s	--	13	--	10 <sup>5</sup> Hz to 0.5 mHz W/kg 45 <sup>0</sup> Ri = 1.2 Ω ; 0.6 V 1.5 Ω ; - 0.4 V 2.5 Ω ; 1 M KCl
[176]	Electrochemical method 0.1 M pyrrole in DW + GO, Sodium perchloride (NaClO <sub>4</sub> ), Pyrrole monomer, gold electrode, scanning rate 100 mV/s, Potc.: - 0.2 to 0.8 V (SCE).	GO/ PPy FE SEM: highly, Porous horn-like, structure.	1 M H <sub>2</sub> SO <sub>4</sub>	424 1 A/g	--	--	--	100 kHz to 10 mHz OCP : 10 mV, 90 <sup>0</sup>
[177]	Electrochemical method AC, Aniline monomer, XPS, AC-Pan, TGA: 200 – 400 <sup>0</sup> C	AC - PAn, AC- MO - PAn FTIR,	0.5 M H <sub>2</sub> SO <sub>4</sub> N <sub>2</sub> bubbled	290.7 390.49 10 mV/s	SE and SP are higher than AC - PAn	--	--	100 kHz to 10 mHz OCP: 10 mV, 90 <sup>0</sup> DW and HCl

450 – 600<sup>0</sup> C mass losses

Scanning rate 10 to 100 mV/s,

Potc.: - 0.2 to 0.8 V (SCE).

- |       |  |   |                                |                |   |   |
|-------|--|---|--------------------------------|----------------|---|---|
| [178] | Hummers method<br>1 mmol aniline,<br>mL tetrabutyl titanate (Ti(OBu) <sub>4</sub> )<br>20 mg GO and,<br>1 mmol (NH <sub>4</sub> ) <sub>2</sub> S <sub>2</sub> O <sub>8</sub><br>In 1 M HCl (30 mL)<br>TGA: 150 to 900 <sup>0</sup> C,<br>PANi completely decompose,<br>scanning rate 10 to 100 mV/s,<br>Potc.: - 0.2 to 0.8 V (Ag/AgCl). | PANI/TiO <sub>2</sub> /GO 1 M H <sub>2</sub> SO <sub>4</sub><br>TEM, FTIR,<br>TGA, XRD,<br>amorphous SEM: flake<br>like Graphene<br>rod | 1020<br>2 mV/s<br>430<br>1 A/g | --<br>--<br>-- | 100 kHz to 10 mHz<br>OCP=5mV<br>R <sub>s</sub> and viscosity<br>PANI/TiO <sub>2</sub><br>1.0, 10.1 and 1.2 Ω<br>PANI/TiO <sub>2</sub> /GO<br>8.1, 9226 and 42.6 Ω | 2 |
| [179] | Novel and Simple method<br>polyaniline,<br>NH <sub>3</sub> -activation was conducted<br>tubular furnace,<br>N <sub>2</sub> and NH <sub>3</sub> at a<br>volume ratio of 1:1 for 1 h,<br>flow of NH <sub>3</sub> was sustained,<br>at 500 <sup>0</sup> C, scanning rate<br>10 to 500 mV/s,<br>PD.: 0.0 to 0.9 V (Ag/AgCl).                 | PANI/TiO <sub>2</sub> /GO 1 M Na <sub>2</sub> SO <sub>4</sub><br>TEM : XPS,<br>XRD : crystalline,<br>SEM: randomly shaped<br>warm       | 174.8                          | --<br>--<br>-- | 10 kHz to 10 mHz<br>90 <sup>0</sup>   |   |

[180]	Chemical oxidative polymerization PPy/CM Polypyrrole/conductive mica oxidant and sodium p-toluene sulfonate (STS) + (APS) ethanol, SnO <sub>2</sub> coated mica, silver-gray, powders, scanning rate 10 to 500 mV/s, PD.: - 0.2 to 0.8 V (SCE).	0.5 M Na <sub>2</sub> SO <sub>4</sub> XRD : semi-crystalline, SEM: clusters and granular	197	--	--	--	10 kHz to 10 mHz 90 <sup>0</sup>	
[181]	Chemical oxidative polymerization PPy/CM Polyaniline/multi-walled carbon nanotubes composites of protonic acid doped PANI with MWNTs 1.0 M HCl scanning rate 10 mV/s, PD.: - 0.2 to 0.8 V (SCE).	1 M NaNO <sub>3</sub> XRD: crystalline, SEM: porous fibrous, TEM,	328	--	--	--	10 kHz to 10 mHz 90 <sup>0</sup>	0.4 V R <sub>i</sub> = 0.5 Ω
[182]	Chemical oxidative polymerization 2-D hexagonal mesoporous carbon silica/triblock copolymer/butanol PANI: 0.9 mL of aniline, 20 mL of 1 mol/L sulfuric acid 10 mL of ethanol were dispersed in 50 mL DW stirring for 10 min, 20 mL of 1 mol/L (NH <sub>4</sub> ) <sub>2</sub> S <sub>2</sub> O <sub>8</sub> (APS)	PANI/MC SEM: porous fibrous, FT IR,	1 M H <sub>2</sub> SO <sub>4</sub>	470	76.4	--	--	---

scanning rate 2, 5, 10 and 50 mV/s,

Potc.: - 0.2 to 1 V (SCE).

- |       |   |  |                     |                                |                                |  |
|-------|---|--|---------------------|--------------------------------|--------------------------------|--|
| [183] | Polymerization Process<br>Tetrahydrofuran (THF)<br>water or organic solvents<br>such as benzene, isopropyl alcohol<br>Aniline monomers, HOGP,<br>0.1M of aniline and 1M HCl<br>Scanning rate 50 mV/s,<br>Potc.: 0 to 0.8 V (SCE).   | PPy/CM<br>XRD: crystalline,<br>SEM: porous fibrous,<br>150 nm, | 3 M KCl470<br>5mV/s | -- --<br>5mV/s                 | -- --<br>5mV/s                 | 10 kHz to 10 mHz<br>90 <sup>0</sup><br>0.4 V<br>R <sub>i</sub> = 0.5 Ω |
| [184] | Electrodeposition<br>Preparation of working electrode<br>sulfuric acid and nitric acid (3:1) for 6 h<br>filtered onto the CC to form a<br>isopropyl alcohol Aniline monomers,<br>graphene paper (GP), GP/CC. Both CC and<br>GP/CC, potentiostatically<br>grown on the CC and the GP/CC<br>under 1.2 V vs. Ag/Ag in an acetonitril<br>Scanning rate 50 mV/s,<br>PD.: 0 to 0.8 V (SCE). | PEDOT/GP/CC<br>SEM: sphere-like,<br>porous                     | 3 M KCl328          | -- --<br>scan rate<br>of 50 mV | -- --<br>scan rate<br>of 50 mV | 10 kHz to 10 mHz<br>90 <sup>0</sup><br>0.4 V<br>R <sub>i</sub> = 0.5 Ω |
| [185] | Polymerization Process<br>Aniline, CSA<br>polytetrafluoroethylene   | PPy-NWs/CM<br>SEM-granular                                     | K-3<br>3 M KCl470   | -- --<br>3 M KCl470            | -- --<br>F/g                   | -- --<br>F/g   |

APS, HCl,

Scanning rate 20 mV/s, current  
density 1 A/g.

PD.: - 0.2 to 0.8 V (SCE).

[186]	Galvanostatic method PPy- Cellulose from Cladophora, Sp.algae Iron (III) chloride hex hydrated Sodium chloride, pyrrole, Current density 10 mA/g. GS.: 0 to 0.6 V (Ag/AgCl).	PPy/CladophoraK-3 Sp. Green SEM-nanorods	2 M KCl	32.4	--	--	--	--
[187]	Sol - Gel Method Aniline monomer Inorganic-organic composite 2 g of SnCl <sub>2</sub> .2H <sub>2</sub> O, in 100 ml Of ethanol, dilute HCl Heated at 120 <sup>0</sup> C and calcinated at 400 <sup>0</sup> C for 2 h. Current density 10 mA/g. GS.: 0 to 0.6 V (Ag/AgCl).	FTIR, FESEM spherical shape particle	Polyaniline/SnO <sub>2</sub> 2 M KCl305.3	36.2	1334	96	0.1 Hz to 10 kHz	0.08 Ω
[188]	Polymerization method Aniline monomer Inorganic-organic composite APS, Titania, H <sub>2</sub> SO <sub>4</sub>	PANi/PNR/TiO <sub>2</sub> SEM	2 M H <sub>2</sub> SO <sub>4</sub>	335	--	--	0.01 Hz to 10 <sup>5</sup> Hz	5V, 0.6- 0.3 Ω 45 <sup>0</sup>

Current density 5 mA.

PD.: - 0.2 to 0.8 V (Ag/AgCl).

- |       |   |  |   |       |    |    |  |                            |
|-------|---|--|---|-------|----|----|--|----------------------------|
| [189] | Cyclic voltammetry<br>PPy, lithium perchlorate,<br>Acetonitrile and<br>Ruthenium chloride<br>Temperature less than 5 <sup>0</sup> C<br>AAO template, PPy<br>nanorods electrodes,<br>RuO <sub>x</sub> - PPy nanocomposites,<br>Scanning rate 50 mV/s,<br>current density 0.1 A/g,<br>PD.: - 0.2 to 1. 0 V (Ag/AgCl). | ppy nanorods<br>RuO <sub>x</sub> - PPy | 1 M H <sub>2</sub> SO <sub>4</sub><br>F/g | 681   | -- | -- | --                                     | --                         |
| [190] | Chemical polymerization<br>PPy, 0.25 M FeCl <sub>3</sub> , <sub>x</sub> H <sub>2</sub> O<br>alcohol solution<br>0, 1, 4 mg RuCl <sub>3</sub> . <sub>x</sub> H <sub>2</sub> O<br>Stirrer the solution 24 h.<br>Scanning rate 5 mV/s,<br>PD.: - 0.4 to 0.6 V (SCE).   | RuO/PPy<br>SEM, TEM                    | 1 M NaNO <sub>3</sub><br>F/g              | 184.6 | -- | -- | 10 <sup>4</sup> to 10 <sup>-2</sup> Hz | 5 mV<br>1.5, 1.7 and 1.8 Ω |

**References**

- [1] B.E. Conway, *Electrochemical Supercapacitors: Scientific, Fundamentals, and Technological Applications*. Kluwer, New York, (1999).
- [2] J.R. Miller, A.F. Burke, *Electrochem. Soc. Interface* 53, 2008.
- [3] A.G. Pandolfo, A.F. Hollenkamp, *J of Power Sources* 157, 27 (2006).
- [4] O. Haas, J. Elton. Cairns, *Annu. Rep. Prog. Chem. Sect. C* 95, 198 (1999).
- [5] X. Andrieu, *Energy Storage Syst. Electron. New Trends Electrochem. Technol.* 1, 521 (2000).
- [6] K. Naoi, P. Simon, *Electrochem. Soc. Interface* (spring, 34 (2008).
- [7] G. Hodes, *Chemical Solution Deposition of Semiconductor Films*. Marcel Dekker Inc., New York (2001).
- [8] M. Nakamura, M. Nakanishi, K. Yamamoto, *J. of Power Sources* 60, 231 (1996).
- [9] P. Simon, A. Burke, *Electrochem. Soc. Interface* (Spring 2008) 38.
- [10] A. Chu, P. Braatz, *J. of Power Source*, 112, 246 (2002).
- [11] E. Karden, Ph.D. dissertation, ISEA, RWTH Aachen, Aachen, Germany, (2001).
- [12] E. Karden, S. Buller, and R. W. De Doncker, *J. of Power Sources* 85, 78 (2000).
- [13] S. Buller, E. Karden, D. Kok, and R. W. De Doncker, *IEEE Trans. Ind. Appl.*,38, no. 6, 1622–1626, (2002).
- [14] E. Barsoukov, J. Ross Macdonald, *Impedance Spectroscopy Theory, Experiment, and Applications*, Second Edition, 2005.
- [15] S. Buller, Ph.D. dissertation, ISEA, RWTH Aachen, Aachen, Germany, 2003.
- [16] Y. Wang, Z.Q. Shi, Y. Huang, Y.F. Ma, C.Y. Wang, M.M. Chen, Y.S. Chen, *J. of Phys. Chem. C* 113, 13103 (2009).
- [17] C. Lin, J.A. Ritter, B.N. Popov, *J. of Electrochem. Soc.* 145, 4097 (1998).
- [18] V. Srinivasan, J.W. Weidner, *J. of Power Sources* 108, 20 (2002).
- [19] X. F. Wang, Y. Zheng, D. B. Ruan, *Chin. J. of Chem.* 24, 1132 (2006).
- [20] H. Kim, T. Seong, J. Lim, W. Cho, *J. of Power Sources* 102, 171 (2001).

- [21] Y. Shan, L. Gao Mater, Chem. Phys. 103 (2007) 210.
- [22] Y. Li, K. Huang, Zufu yao, Suqin Liu, Xiaoxia Qing, Electrochimica Acta, 56, 2144 (2011).
- [23] S.G. Kandalkar, J. L. Gunjekar, C.D. Lokhande, Appl. Surf. Sci. 254, 5544 (2008).
- [24] T. Brousse, D. Bélanger, Electrochem. Solid-State Lett. 6, A248 (2003).
- [25] B.E. Conway, J. of Electrochem. Soc. 138, 1548 (1991).
- [26] J.P. Zheng, T.R. Jow, J. of Electrochem. Soc. 142, 6 (1995).
- [27] H. K. Kim, T. Y. Seong, J. H. Lim, Y. W. Ok, W. I. Cho, Y.H. Shin, Y.S. Yoon, J. Vac. Sci. Technol. B 20 (5), 1827 (2002).
- [28] Y.S. Yoon, W.I. Cho, J.H. Lim, D.J. Choi, J. of Power Sources, 101, 129 (2001).
- [29] J.H. Lim, D.J. Choi, H.-K. Kim, W.I. Cho, Y.S. Yoon, J. of Electrochem. Soc. 148, 275 (2001).
- [30] U.M. Patil, S.B. Kulkarni, V.S. Jamadade, C.D. Lokhande, J of Alloys and Compounds, 509, 1682 (2011).
- [31] W. C. Fang, J. H. Huang, L. C. Chen, Y. Long Oliver Su, K. H. Chen, J. of Power Sources 160, 1510 (2006).
- [32] V.D. Patake, C.D. Lokhande, Oh Shim Joo, Applied Surface Science 255, 4196 (2009).
- [33] K. H. Kim, K. S. Kim, G. P. Kim, S. H. Baek, Current Applied Physics, xxx, 4 (2011).
- [34] H. Jong. L. Jang, K. Machida, Y. Kim, K. Naoi, Electrochimica Acta 52, 1741 (2006).
- [35] Li-Ming Huang, Hong-Ze Lin, Ten-Chin Wen, A. Gopalan, Electrochimica Acta 52, 1063 (2006).
- [36] V.D. Patake, C.D. Lokhande, Applied Surface Science 254, 2824 (2008).
- [37] Y. Sato, K. Yomogida, T. Nanaumi, K. Kobayakawa, Y. Ohsawa, M. Kawai, Electrochem. Solid State Lett. 3, 113 (2000).
- [38] C. Lin, J.A. Ritter, B.N. Popov, J. Electrochem. Soc. 146, 3155 (1999).
- [39] Y. Takasu, T. Nakamura, H. Ohkawauchi, Y. Murakami, J. Electrochem. Soc. 144, 2601 (1997).
- [40] I. Zhitomirsky, L. Gal-Or, Mater. Lett. 31, 159 (1997).
- [41] Y. G. Wang, Z. D. Wang, Y. Y. Xia, Electrochimica Acta 50, 5646 (2005).
- [42] B. Messaoudi, S. Joiret, M. Keddou, H. Takenouti, Electrochim. Acta 46, 2498 (2001).

- [43] T. C. Wen, C. C. Hu, Y. J. Lee, *J. Electrochem. Soc.* 140, 2554 (1993).
- [44] C. C. Hu, C. Y. Hung, K. H. Chang, Y. L. Yang, *J. of Power Sources* 196, 850. (2011).
- [45] D. P. Dubal, A. D. Jagadale, C. D. Lokhande, *Electrochimica Acta* 80, 170 (2012).
- [46] P. K. Nayak, N. Munichandraiah, *Microporous and Mesoporous Materials* 143, 214 (2011).
- [47] T. Yousefi, A. N. Golikand, M. H. Mashhadizadeh, M. Aghazadeh, *Current Applied Physics* xxx, 6 (2011).
- [48] Zhongchun Li, Hongling Bao, Xiaoyu Miao, Xuhong Chen, *J. of Colloid and Interface Science* 357, 291 (2011).
- [49] D.P. Dubal, D.S. Dhawale, T.P. Gujar, C.D. Lokhande, *Applied Surface Science* 257, 3382 (2011).
- [50] Y. Li, H. Xie, J. Wang, L. Chen, *Materials Letters* 65, 405 (2011).
- [51] C. C. Hu, C. Y. Hung, K. H. Chang, Y. L. Yang, *J. of Power Sources* 196, 850 (2011).
- [52] J. M. Koa, K. M. Kim, *Materials Chemistry and Physics*, 114, 841 (2009).
- [53] T. Nathan, A. Aziz, A.F. Noor, S.R.S. Prabakaran, *J. Solid State Electrochem.* 12, 1009 (2008).
- [54] D. Zhao, W. Zhou, H. Li, *Chem. Mater.* 19, 3882 (2007).
- [55] J. W. Lee, T. Ahn, J. H. Kim, J. M. Ko, J. D. Kim, *Electrochimica Acta* 56, 4857 (2011).
- [56] T.W. Kim, S.-J. Hwang, S.H. Jhung, J.-S. Chang, H. Park, W. Choi, J.H. Choy, *Adv. Mater.* 20, 542 (2008).
- [57] J.S.E.M. Svensson, C.G. Granqvist, *Appl. Phys. Lett.* 49, 1568 (2009).
- [58] B. Varghese, M.V. Reddy, Y.W. Zhu, C.S. Lit, T.C. Hoong, G.V. Subba Rao, B.V.R. Chowdari, A.T.S. Wee, C.T. Lim, C.-H. Sow, *Chem. Mater.* 20, 3367 (2008).
- [59] X. Li, J.P. Liu, X.X. Ji, J. Jiang, R.M. Ding, Y.Y. Hu, A.Z. Hu, X.T. Huang, *Sens. Actuators B* 147, 247 (2010).
- [60] D.Y. Han, H.Y. Yang, C.B. Shen, X. Zhou, F.H. Wang, *Powder Technol.* 147, 116 (2004).
- [61] C.K. Xu, K.Q. Hong, S. Liu, G.H. Wang, X.N. Zhao, *J. of Cryst. Growth* 255, 312. (2003).

- [62] Y.J. Zhan, C.R. Yin, C.L. Zheng, W.Z. Wang, G.H. Wang, *J. of Solid State Chem.* 177, 2284 (2004).
- [63] H.A. Pang, Q.Y. Lu, Y.Z. Zhang, Y.C. Li, F. Gao, *Nanoscale* 2, 922 (2010).
- [64] W.Z. Wang, Y.K. Liu, C.K. Xu, C.L. Zheng, G.H. Wang, *Chem. Phys. Lett.* 362,122. (2002).
- [65] S.A. Needham, G.X. Wang, H.K. Liu, *J. of Power Sources* 159, 257 (2006).
- [66] X. M. Ni, Y.F. Zhang, D.Y. Tian, H.G. Zheng, X.W. Wang, *J. of Cryst. Growth* 306, 421 (2007).
- [67] M. Zhang, G.J. Yan, Y.G. Hou, C.H. Wang, *J. of Solid State Chem.* 182, 1210 (2009).
- [68] W. Zhou, L. Ge, Z. Chen, F. Liang, H. Xu, J. Motuzas, A. Julbe, Z. Zhu, *Chemistry of Materials* 23, 4198 (2011).
- [69] G.X. Pan, X. Xia, F. Cao, P.S. Tang, H.F. Chen, *Electrochimica Acta* 63, 340 (2012).
- [70] J. Gemmer, Y. Hinrichsen, A. Abel, Bachmann, *J. of Journal of Catalysis* 290, 224 (2012).
- [71] L. Wang, H.W. Xu, P.C. Chen, D.W. Zhang, C.X. Ding, C.H. *J. of Power Sources* 193, 850 (2009).
- [72] P.S. Patil, C.D. Lokhande, S.H. Pawar, *J. Phys. D., Appl. Phys.* 22, 550 (1989).
- [73] S.H. Pawar, P.S. Patil, R.D. Madhal, C.D. Lokhande, *Indian J. Pure and Appl. Phys.* 27, 230 (1989).
- [74] M. Buchler, P. Schmuki, H. Bo hni, *J. of Electrochem. Soc.* 145, 614 (1998).
- [75] M.F. Toney, A.J. Davenport, L.J. Oblonsky, M.P. Ryan, C.M. Vitus, *Phys. Rev. Lett.* 79, 4282 (1997).
- [76] W. H. Jin, G. T. Cao, J. Y. Sun, *J. of Power Sources*, 175, 691 (2008).
- [77] J. S. Shaikh, R. C. Pawar, P.S. Patil, A.V. Moholkar, J.H. Kim., *Applied surface science*, 257, 4397 (2011).
- [78] J. S.Shaikh, R. C. Pawar, P.S. Patil, D.S. Patil N.L.Taarwal, *J. of alloys and compound* 509, 7174 (2011).
- [79] Y. Liu, X. Tian, Yan, Y., *Canadian J. of Chemistry*, 90, 525 (2012).
- [80] Y. Qi, N. Du, H. Zhang, Wang, J., Yang, Y., Yang, D., *J. of Alloys and Compounds* 521, 89 (2012).
- [81] S. Choi, Manthiram, A. *J. of the J. of Electrochem. Society* 149, 573 (2002).
- [82] V.D. Patake, S.S. Joshi, C.D. Lokhande, Oh shim Joo, *Materials Chemistry and Physics* 114, 9 [2009].
- [83] W. M Jin, J. H.Kang, Moon, J.H., *ACS Applied Materials and Interfaces*, 2, 2986 (2010).

- [84] G. Wang, J. C. Hunang, S. Chen, Y. Gao, D. CuO, *J. of power source* 5760, (2011).
- [85] D. W. Kim, K. Y. Rhee, S. J. Park, *J. of Alloys and Compounds* 530, 10 (2012).
- [86] C. C. Hu, C. M. Huang, K. H. Chang, *J. of Power Sources* 185, 1597 (2008).
- [87] D.W. Murphy, P.A. Christian, F.J. Disalo, J.N. Carides, *J. Electrochem. Soc.* 126, 499 (1979).
- [88] H. M. Zheng, Y. Zhao, Y.J. Hao, Q.Y. Lai, J.H. Huang, X.Y. Ji, *J. of Alloys and Compounds* 477, 804 (2009).
- [89] D.W. Choi, G.E. Blomgren, P.N. Kumta, *Adv. Mater.* 18, 1178 (2006).
- [90] D.W. Choi, P.N. Kumta, *J. Electrochem. Solid-State Lett.* 8, A418 (2005).
- [91] C. H. Lai, C. K. Lin, S. W. Lee, H. Y. Li, J. K. Chang, M. J. Deng, *J. of Alloys and Compounds* xxx (2011).
- [92] S.N. Pusawale, P.R. Deshmukh, C.D. Lokhande, *Applied Surface Science* xxx (2011).
- [93] Z. J. Li, T.X. Chang, G.Q. Yun, Y. Jia, *Powder Technology* 224, 310 (2012).
- [94] I. Shakir, M. Shahid, M. Nadeem, D. J. Kang, *Electrochimica Acta* 72, 137 (2012).
- [95] Z.R. Dai, Z.W. Pan, Z.L. Wang, *Adv. Funct. Mater.* 13, 9 (2003).
- [96] Z.Y. Yuan, B.L. Su, *Colloid Surf. A-Physicochem. Eng. Aspects* 241, 173 (2004).
- [97] X.S. Peng, A.C. Chen, *Adv. Funct. Mater.* 16, 1355 (2006).
- [98] J. H. Jung, H. Kobayashi, K.J.C. van Bommel, S. Shinkai, T. Shimizu, *Chem. Mater.* 14, 1445 (2002).
- [99] Y. Xie, C. Huang, L. Zhou, Y. Liu, H. Huang, *Composites Science and Technology* 69, 2114. (2009).
- [100] C. C. Hu, H. Y. Guo, K. H. Chang, C. C. Huang, *Electrochemistry Communications* 11, 1634 (2009).
- [101] R. Giovanardi, G. Orlando, *Surface and coatings technology* (2011).
- [102] E. Frackowiak, V. Khomenko, K. Jurewicz, K. Lota, F. Beguin, *J. of Power Sources* 153, 413 (2006).
- [103] F. Beguin, K. Szostak, G. Lota, E. Frackowiak, *Adv. Mater.* 17, 238 (2005).
- [104] E. Raymundo-Pinero, V. Khomenko, E. Frackowiak, F. Beguin, *J. of Electrochem. Soc.* 152, A229 (2005).
- [105] J. Orkans, M.W. Shafer, *J. of Electrochem. Soc.* 124, 1202 (1977).

- [106] S. Hackwood, G. Geni, M.A. Bosch, K. Kang Phys. Rev. B 26, 7073 (1982).
- [107] M. Blouion, D. Guay, J. of Electrochem. Soc. 144, 573 (1997).
- [108] G. Lota, E. Frackowiak, J. Mittal, M. Monthieux, Chemical Physics Letters 434, 77 (2007).
- [109] J. Chang, R. S. Mane, D. Ham, W. Lee, Electrochimica Acta 53, 699 (2007).
- [110] J. Chang, V. V. Todkar, R. S. Mane, D. Ham, Physics E 41, 1745 (2009).
- [111] A. Chu, P. Braatz, J. Power Sources 112 (2002).
- [112] D. Kalpana, K.S. Omkumar, S. Suresh Kumar, N.G. Renganathan, Electrochimica Acta 52, 1315 (2006).
- [113] B. McEnaney, T.D. Burchell (Eds.), Carbon Materials for Advanced Technologies, Pergamon 1, (1999).
- [114] H.O. Pierson, Handbook of Carbon, Graphite, Diamond and Fullerenes, Noyes Publications, NJ, USA, 1993.
- [115] M. Inagaki, H. Konno, O. Tanaike, Journal of Power Sources 195, 7903 (2010).
- [116] A Graeme. Snooka, Pon Kao, Adam S. Best, J. of Power Sources 196, 12 (2011).
- [117] R. McNeill, D.E. Weiss, J.H. Wardlaw, R. Siudak, Aust. J. Chem. 16, 1056 (1963).
- [118] B.A. Bolto, D.E. Weiss, Aust. J. of Chem. 16, 1076 (1963).
- [119] B.A. Bolto, R. McNeill, D.E. Weiss, Aust. J. of Chem. 16, 1090 (1963).
- [120] T. C. Wen, C.-C. Hu, Y.-J. Lee, J. of Electrochem. Soc. 140, 2554 (1993).
- [121] C.Y. Chu, J. T. Tsai, C.L. Sun, International J. of Hydrogen Energy xxx, 7 (2012).
- [122] J. M. Luo, B. Gao, X. G. Zhang, Materials Research Bulletin, 43, 1125 (2008).
- [123] Y. Xie, D. Fu, Material Chemistry and Physics, 122, 29 (2010).
- [124] S. H. Choi, J. S. Kim, Y. S. Yoon, Electrochimica Acta, 50, 552 (2004).
- [125] V. Gupta, S. Gupta, N. Miura, J. of Power Source, 175, 685 (2008).
- [126] G. X. Pan, X. Xia, F. Cao, P.S. Tang, H.F. Chen, Electrochimica Acta, xx (2012).
- [127] V. Gupta, T. Kawaguchi, N. Miura, Material Research Bulletin, 44, 206 (2009).

- [128] G. Wang, Lei Zhang, Jenny Kim, JiuJun Zhang, *J. of Power Source*, xx (2011).
- [129] A. R. Souza, E. Arashiro, H. Golvei, T. A.F. Lassali, *Electrochimica Acta*, 49, 2023 (2004).
- [130] Q. Wang, L. Jiao, H. Du, Q. Huan, W. Peng, D. Song, Y. Wang, H. Yuan, *Electrochimica Acta* 58, 441 (2011).
- [131] G. He, J. Li, H. Chen, J. Shi, X. Sun, S. Chen, X. Wang, *Materials Letters* 82, 63 (2012).
- [132] Y. Yu Liang, Lin Cao, ling- Bin Kong, Hu-Lin Li, *J. of Power Source* 136 200 (2004) 197 –.
- [133] Z. Fan, J. Chen, K. Cui, F. Sun, Y. Xu, Y. Kuang, *Electrochimica Acta* 52, 2665 (2007).
- [134] Q. Chu, W.Wang, X. Wang, B. Yang, X. Liu, J. Chen, *J. of Power Sources* 276, 25 (2015).
- [135] S. K. Chang, Z. Zainal, K. B.Tan, N. Yusof, W. M. Daud W. Yusoff, S.R.S. Prabaharan, *Current Applied Physics* xx, 1 (2012)
- [136] M. Asgari, M. G. Maragheh, R. Davarkhah, E. Lohrasbi, A. N. Golikand, *Electrochimica Acta*, 59, 289 (2012).
- [137] R. R. Salunkhe, K. Jang , H. Yu, S. Yu, T. Ganesh, S. H. Han, H. Ahna, *J. of Alloys and Compounds* 509, 6682 (2011).
- [138] D.P. Dubal, A.D. Jagadale, S.V. Patil, C.D. Lokhande, *Material Research Bulletin* 47, 1245 (2012).
- [139] J. M. Luo, B. Gao, X. G. Zhang, *Material Research bulletin* 43, 1125 (2008).
- [140] Ka. Yokoshim, T. Shibutani, M. Hirot, W. Sugimoto, Y. Murakami, Y. Takasu, *J. of Power Sources* 160, 1486 (2006).
- [141] H. K. Kim, S. H. Choi, Y. S. Yoon, S. Y. Chang, Y. W. Okd, T. Y. Seong, *Thin Solid Films* 475, 57 (2005).
- [142] C. D. Lokhande, B. O. Park, H. S. Park, K. D. Jung, O. S. Joo, *Ultramicroscopy* 105, 274 (2005).
- [143] W. Y. Gang, Z. X. Gang, *Electrochemical Acta* 49, 1962 (2004).
- [144] Y. Xie, C. Huang, L. Zhou, Y. Liu, H. Huang, *Composites Science and Technology*, 69, 2114 (2009).
- [145] B. J. Lee, S. R. Sivakkumar, J. M. Ko, J. H. Kim, S. M. Jo, D. Y. Kim, *J. of Power Sources* 168, 552 (2007).
- [146] M. Jaylakshmi, M. Mohan Rao, N. Venugopal, K. B. Kim, *J. of Power Source* 166, 583 (2007).
- [147] J. Lang, X. Yan, Q. Xue, *J. of Power Source* 196, 7846 (2011).
- [148] X. J. He, Y.J. Geng, S. Oke, K. Higashi, M. Yamamoto, H. Takikaw, *Synthetic Metals* 159, 12 (2009).

- [149] S. K. Chang, Z. Zainal, K. B. Tan, N. A. Yusof, W. M. D. Wan Yusoff, S. R. S. Prabakaran, *Current Applied Physics* xxx, 8 (2012).
- [150] J. Yan, T. Wei, W. Qiao, B. Shao, Q. Zhao, L. Zhang, Z. Fan, *Electrochimica Acta* 55, 6978 (2010).
- [151] M. Asgari, M. G. Maragheh, R. Davarkhah, E. Iohrasbi, A. N. Golikand, *Electrochimica Acta* 59, 289 (2012).
- [152] Z. Fan, J. Zhen, K. Cui, F. Sun, Y. Xu, Y. Kuang, *Electrochimica Acta* 52, 2965 (2007).
- [153] T. Lu, Y. Zhang, H. Li, L. Pan, Y. Li, Z. Sun, *Electrochimica Acta* 55, 4173 (2010).
- [154] L. Wang, D. L. Wang, *Electrochimica Acta* 56, 5015 (2011).
- [155] J. Li, Q. M. Yang, I. Zhitomirsky, *J. of Power Source* 185, 1574 (2008).
- [156] C. Y. Chen, T. C. Chien, Y. C. Chan, C. K. Lin, S. C. Wang, *Diamond and Related Materials* 18, 485 (2009).
- [157] Z. Li, J. Wang, S. Liu, X. Liu, S. Yang, *J. of Power Sources* 196, 8165 (2011).
- [158] S. B. Ma, K. W. Nam, W. S. Yoon, X. Q. Yang, K. Y. Ahn, K. H. Oh, K. B. Kim, *Electrochemistry Communications* 9, 2811 (2007).
- [159] E. H. Liu, X. Y. Meng, R. Ding, J. C. Zhou, S. T. Tan, *Materials Letters* 61, 3489 (2007).
- [160] X. J. He, Y. J. Geng, S. Oke, K. Higashi, M. Yamamoto, H. Takikawa, *Synthetic Metal* 159, 12 (2009).
- [161] V. V. Panic, A. B. Dekanski, R. M. Stevanovic, *J. of Power source* 195, 3976 (2010).
- [162] M. Jayalakshmi, M. Mohan Rao, N. Venugopal, Kwang-Bum Kim, *J. of Power Source* 166, 583 (2007).
- [163] T. Kudo, Y. Ikeda, T. Watanabe, M. Hibino, M. Miyayama, H. Abe, K. Kajita, *Solid State Ionics* 153, 841 (2002).
- [164] Z. Lei, D. Bai, X. S. Zhao, *Microporous and Mesoporous Materials* xxx, xxx (2011).
- [165] R. B. Rakhi, H. N. Alshareef, *J. of Power Source*, 196, 8865 (2011).
- [166] Y. Wu, R. Balakrishna, M. V. Reddy, A. Sreekumaran Nair, B. V. R. Chowdari, S. Ramakrishna, *J. of Alloys and Compounds* 517, 74 (2012).
- [167] Y. H. Kim, S. J. Park, *Current Applied Physics* 11, 466 (2011).

- [168] E. Frackowiak, V. Khomenko, K. Jurewicz, K. Lota, F. Beguin, *J. of Power Sources* 153, 418 (2006)
- [169] Z. A. Hu, Y. L. Xie, Y. X. Wang, L. P. Mo, Y. Y. Yang, Z. Y. Zhang, *Materials Chemistry and Physics* 114, 995 (2009).
- [170] H. Xu, Q. Cao, X. Wang, W. Li, X. Li, H. Deng, *Materials Science and Engineering B* 171, 108 (2010).
- [171] M. Yang, B. Cheng, H. Song, X. Chen, *Electrochimica Acta*, 55, 7027 (2010).
- [172] J. J. Cai, L. B. Kong, J. Zhang, Y. C. Luo, L. Kang, *Chinese Chemical Letters*, 21, 1512 (2010).
- [173] J. Yan, T. Wei, W. Qiao, Z. Fan, L. Zhang, T. Li, Q. Zhao, *Electrochemistry communications*, 12, 1282 (2010).
- [174] Y. Hu, Y. Zhao, Y. Li, H. Li, H. Shao, L. Qu, *Electrochimica Acta*, 66, 286 (2012).
- [175] J. Wang, Y. Xu, X. Chen, X. Du, *J. of Power Sources*, 163, 1125 (2007).
- [176] H. H. Chang, C. K. Chang, Y. C. Tsai, C. S. Liao, *Carbon*, 50, 2336 (2012).
- [177] Y. Jia, J. Jiang, K. Sun, T. Dai, *Electrochimica Acta* 71, 218 (2012).
- [178] H. Su, T. Wang, S. Zhang, J. Song, C. Mao, H. Niu, B. Jin, J. Wu, Y. Tian, *Solid State Sciences* 14, 681 (2012).
- [179] N. D. Kim, S. J. Kim, G. P. Kim, I. Nama, H. Jin Yun, P. Kim, J. Yi, *Electrochimica Acta* 78, 346 (2012).
- [180] C. Yang, P. Liu, *Synthetic Metals*, 160, 773 (2010).
- [181] B. Dong, B. L. He, C. L. Xu, H. L. Li, *Materials Science and Engineering, B* 143, 13 (2007).
- [182] S. H. Zhou, S. Mo, W. Zou, F. Jiang, T. Zhou, D. Yuan, *Synthetic Metals* 161, 1628 (2011)
- [183] Q. Liu, M. H. Nayfeh, S. T. Yau, *J. of Power Sources*, 195, 3959 (2010).
- [184] C. Y. Chu, J. T. Tsai, C. L. Sun, *International Journal of Hydrogen Energy* xxx, 7 (2012).
- [185] H. K. Kim, S. H. Choi, Y. S. Yoon, S. Y. Chang, Y. W. Ok, T. Y. Seong, *Thin Solid Films* 475, 57 (2005).
- [186] H. Olsson, G. Nystrom, M. Stromme, M. Sjodin, L. Nyholm, *Electrochemistry communication* 13 871 (2011).
- [187] Z. A. Hu, Y. L. Xie, Y. X. Wang, L. P. Mo, Y. Ying, Z. Y. Zhang, *Materials Chemistry and Physics* 114 995, (2009).
- [188] H. Xu, Q. Cao, X. Wang, W. Li, X. Li, H. Deng, *Materials Science and Engineering, B* 171, 108 (2010).
- [189] H. Lee, M. S. Cho, H. Kim, J. D. Nam, Y. K. Lee, *Synthetic Metal* 160, 1059 (2010).

[190] B. L. He, Y. K.Zhou, W.J. Zhou, B. Dong, H. L. Li, M. Science and Engineering A 374, 326 (2004).